SILK FIBROIN FILMS FOR CORNEAL TISSUE ENGINEERING APPLICATION: A PROCESS - PROPERTY RELATIONSHIP STUDY

A DISSERTATION SUBMITTED BY

Ms. MAYA B

2019/M Phil/04

IN PARTIAL FULFILLMENT OF THE REQUIREMENTS FOR THE AWARD OF

MASTER OF PHILOSOPHY

IN

BIOMEDICAL TECHNOLOGY

SREE CHITRA TIRUNAL INSTITUTE FOR MEDICAL SCIENCES AND TECHNOLOGY, THIRUVANANTHAPURAM – 695011

JULY 2020

DECLARATION

I, **Maya B**, hereby declare that I had personally carried out the work depicted in the thesis entitled, **"Silk fibroin films for corneal tissue engineering application: a process - property relationship study"** under the direct supervision of **Dr. Naresh Kasoju**, Scientist-C (Applied Biology), Division of Tissue Culture, Department of Applied Biology, Biomedical Technology Wing, Sree Chitra Tirunal Institute for Medical Sciences and Technology, Thiruvananthapuram, Kerala, India.

Thiruvananthapuram

Date: 21-07-2020

Ms. Maya B

2019/M Phil/04

SREE CHITRA TIRUNAL INSTITUTE FOR MEDICAL SCIENCES AND TECHNOLOGY, THIRUVANANTHAPURAM – 695011, INDIA

(An Institute of National Importance under Dept. of Science and Technology, Govt. of India with the status of University by an Act of Parliament in 1980)

CERTIFICATE

This is to certify that the dissertation entitled **"Silk fibroin films for corneal tissue engineering application: a process - property relationship study"** is a bonafide work done by **Ms. Maya B** (Reg. No. 2019/ MPhil /04) in partial fulfilment for the degree of **Master in Philosophy** in **Biomedical Technology** under my supervision and guidance at **Division of Tissue Culture**, Biomedical Technology Wing, Sree Chitra Tirunal Institute for Medical Sciences and Technology, Thiruvananthapuram, Kerala, India.

Thiruvananthapuram
Date: 21-07-2020

Dr. Naresh Kasoju
Scientist-C (Applied Biology)

SREE CHITRA TIRUNAL INSTITUTE FOR MEDICAL SCIENCES AND TECHNOLOGY, THIRUVANANTHAPURAM – 695011, INDIA

(An Institute of National Importance under Dept. of Science and Technology, Govt. of India with the status of University by an Act of Parliament in 1980)

The thesis entitled "**Silk fibroin films for corneal tissue engineering application: a process - property relationship study"** submitted by **Ms. Maya B** (Reg. No. 2019/MPhil/04) for the award of the degree of **Master of Philosophy** in **Biomedical Technology** from **Sree Chitra Tirunal Institute For Medical Sciences and Technology Thiruvananthapuram** was evaluated and approved by

Supervisor

Signature:

Name: Dr. Naresh Kasoju

Date: 21.07.2020

Examiner

Signature:

Name: Dr. REKHA M.R.

Date: 28.07.2020

Contents

Acknowledgement

Here I take the opportunity to express my gratitude to all those who have helped me in completion of my project and in presenting this dissertation in partial fulfillment of the Degree of Master of Philosophy.

I cordially articulate my thanks to Dr. Asha Kishore The Director, SCTIMST, Dr. Harikrishna Varma P R, Head (BMT Wing), Dr. Sankara Sharma P., Dean, Dr. Santhosh Kumar V, Registrar, for the opportunity given and providing the necessary facilities and to complete the course successfully.

I am deeply indebted to my supervising guide Dr. Naresh Kasoju, Scientist C, Division of Tissue Culture, SCTIMST for his guidance and support for the completion of my work. It was a very enriching experience for me all along six months of dissertation work. He allowed me to work with complete intellectual freedom. The encouragement, the inspiration received all through these days will always help me in future.

I would like to express my hearty thanks to Dr. Maya Nandkumar, Head, Department of Applied Biology, Dr. Anil Kumar P R, Scientist-in-Charge, Division of Tissue Culture, Dr Senthil kumar, Dr. Praveen K S and my colleagues Ms. Jimna Mohammad Ameer, Project Assistant, Ms. Athira RK, Project Assistant, Ms. Anju MS, Project assistant and Mr. Febin R Dan, M Tech Student, Division of Tissue Culture, SCTIMST for the timely criticism of work and fruitful discussions. I would like to express a special note of gratitude for their help, suggestions and constant support throughout the study.

I am thankful to all the staffs of Tissue Culture for their support and encouragement. My heartfelt thanks to Mrs. Usha Vasudev, Mrs. Deepa K Raj and Mr. Vinod D for their constant support and encouragement at all time. Special thanks to my lab members, Mrs. Aswathy M R, Mrs. Kavya, Mrs. Asha V Nath, Ms. Anupama Sekhar, Ph D Student, Dr. Remya, Research Associate, Ms. Shilpa Ajith, Project Assistant, Mr. Roopesh R Pai, PhD student, Dr. Eva C Das, PhD Student, Ms. Kripamol R, PhD student, for their valuable support throughout my work.

I express my gratitude to Mrs. Nimy N, Central Analytical for helping me in using contact angle instrument and Mrs. Sasikala TS, Central Analytical Facility for helping me in FTIR analysis. I am also indebted to Mr. Chandra Sekhar Nayak M, Division of Polymeric Medical Devices for his timely help in Tensile strength testing. I gratefully

acknowledge Mr. Nishad KV for his help in Environmental Scanning Electron Microscopy and Mr. Jithu, for his help in surface profilometry analysis.

I am extremely thankful to my batch mates who were with me all the time, understanding, and supporting me whenever I feel discouraged and dejected.

I express my deep sense of gratitude to Dr. Francis Boniface Fernandez and Dr. Jayasree RS, and Dr. Anoop Kumar T, M Phil Coordinators SCTIMST for their academic assistance.

Without the prayer, support, patience, encouragement, love, and care from my family, especially my mother Mrs. K R Beena, I could not have finished my study. I would like to express my gratitude to Mr. Deepu for giving support in finishing this work,

Finally, I humbly bow before the almighty for giving me the strength, wisdom, and luck to complete this dissertation.

List of Abbreviations

APS	Ammonium Per Sulphate
AQ	Aqueous
ATR-FTIR	Attenuated Total Reflection-Fourier Transform Infrared Spectroscopy
DMEM	Dulbecco's Modified Eagle Medium Medium
DSF	Degummed Silk Fibroin
ECM	Extracellular Matrix
EDAX	Energy Dispersive X-ray Spectroscopy
ETO	Ethylene Oxide
FA	Formic Acid
FBS	Fetal Bovine Serum
HFIP	1,1,1,3,3,3-Hexafluoro-2-propanol
ISO	International Organization for Standardization
LiBr	Lithium Bromide
MTT	3-(4,5-dimethylthiazol-2-yl)-2,5-diphenyl tetrazolium bromide
OD	Optical Density
PAGE	Poly Acrylamide Gel Electrophoresis
PBS	Phosphate Buffered Saline
RSF	Reconstituted Silk Fibroin
SD	Standard Deviation
SDS	Sodium Dodecyl Sulphate
SEM	Scanning Electron Microscopy
SF	Silk Fibroin
STF	Simulated Tear Fluid
TCPS	Tissue Culture Polystyrene Plates
TE	Tissue Engineering
UV-VIS	ultraviolet-visible

List of Notations

µg	Microgram
%	Percentage
°C	Degree Celsius
µl	Microliter
µm	Micrometer
cm^2	Centimeter square
g or gm	Gram
h or hrs	Hours
KDa	Kilo Dalton
KeV	Kilo electron Volt
KV	Kilo Volt
L	Liter
M	Molar
Min	Minute
Ml	Milliliter
Mm	Millimeter
mm^2	Millimeter square
Nm	Nanometer
Rpm	Rotation per minute
Rq	Root mean square deviation
Sec	Second
U	Unit
V	Volt
A	Alpha
B	Beta

List of Figures

List of Tables

Synopsis

Cornea is a clear and transparent part of eye on its anterior portion and is responsible for two third of eye's optical power. It is estimated that over 10 million individuals experience corneal blindness worldwide due to diseases, age related problems, accidents, etc. Currently, corneal transplantation is the only possible method to restore vision, however, shortage of donors, risk of infections and rejection rates made researchers to find an alternative method. To this end, tissue engineering has become a remedial method which involves regeneration of bio-artificial tissues *in vitro* by culturing cells of patients or healthy donors on a scaffold in presence of bioactive growth factors. However, the two major challenges in the field of tissue engineering in constructing a cornea are: transparency and tissue strength. There are a variety of materials that are being tested as corneal scaffold, *Bombyx mori* silkworm derived silk fibroin is a recent addition to this list. The journey of silk as a biomedical material began in the 19th century because of its robust track record for non-toxicity, slow biodegradability, processing features and excellent mechanical properties. However, its use in the field of corneal tissue engineering is very limited, as evident from literature reports in scientific indexing websites. Further, irrespective of tissue of choice, there was no study till date to investigate process dependent variations in silk biomaterials.

To this end, here we formulated the current study with an aim to fabricate *B. mori* silk fibroin films and to investigate whether or not the processing parameters show any variations on its morpho - topological, physico - chemical, optical and biological properties. For this purpose, we have set the following objectives: (a) to degum *Bombyx mori* silk cocoons into silk fibroin fibres and characterized its morphological and chemical/structural properties, (b) to reconstitute the degummed fibres into aqueous silk fibroin solution and characterize its molecular weight and chemical/structural properties, (c) to process RSF (reconstituted silk fibroin) solution in AQ (Aqueous), FA (Formic acid) and HFIP (1,1,1,3,3,3-Hexa fluoro isopropanol) into films by solvent casting approach, followed by annealing with methanol, water and steam, and to characterize its morphological properties (SEM- scanning electron microscopy, surface roughness), physical properties (contact angle, swelling index, water uptake, water vapor transmission%), chemical/structural properties (FTIR- Fourier transform infrared spectroscopy), optical properties (optical clarity, absorbance spectra and transmission% in UV-Visible range), degradation properties, (d) finally, to evaluate its cytotoxicity with

L929 cells and cytocompatibility with SIRC (rabbit corneal) cells to determine its potential application in corneal tissue engineering.

This thesis consists of 4 chapters viz. (1) Introduction and Review of Literature, (2) Materials and Methods, (3) Results and Discussion, (4) Conclusion and Future Prospects.

Chapter 1 includes brief introduction to the work, followed by comprehensive review of literature on sources of silk fibroin, structure and composition of silk fibroin, fundamentals of tissue engineering, silk fibroin as a scaffolding biomaterial, silk fibroin in various tissue engineering applications, corneal anatomy and physiology, corneal tissue engineering and regenerative medicine, silk fibroin as a biomaterial in corneal regeneration, process – property relationships in silk fibroin biomaterials. This is followed by details on research gap analysis, hypothesis, aim and objectives.

Chapter 2 describes details of materials used in the study, followed by methods adopted to achieve the objectives viz. preparation and characterization of degummed silk fibroin (DSF), preparation and characterization of RSF, fabrication and post-fabrication processing of RSF films and subsequent characterization including its morpho-topological, physico-chemical, optical, and biological properties. Further, we describe methods to evaluate its cytotoxicity with L929 cells and cytocompatibility with SIRC cells to determine its potential application in corneal tissue engineering.

Chapter 3 describes results of morpho-chemical properties of DSF, molecular weight and chemical properties of RSF, successful processing of RSF solution in AQ, FA and HFIP into films by solvent casting approach with and without annealing in methanol, water and steam, and its morphological properties (SEM, surface roughness), physical properties (contact angle, swelling index, water uptake, water vapor transmission%), chemical properties (FTIR), optical properties (optical clarity, absorbance spectra and transmission%), degradation profile, cytotoxicity and cytocompatibility with SIRC cells.

Chapter 4 describes the conclusions of the work which include incidence of process dependent differences in morpho-topological, physico-chemical, optical and degradation properties of RSF films, non - cytotoxic nature of RSF films irrespective of processing conditions, and finally, desirable compatibility of RSF films, irrespective of processing conditions, with corneal cells indicating its application in corneal tissue engineering.

This is followed by a collection of references with complete bibliographic information sited in various chapters of this thesis.

Chapter 1: Introduction and Review of Literature

1.1 Introduction

Eyes are the window to the soul – an expression that flawlessly echoes what we feel when our looks thrust into another. Sight is a sensory experience where in image and vision is created after lights get reflected off from an object and gets focused by eye. Vision - a metaphysical concept, where in the mind interprets these images and help realize the significance of that event, are important phenomenon that allow us to connect with our surroundings. Just as intriguing these phenomena of the eye sounds like, is the complexity of the eye anatomy and its function. It has a number of elements which include cornea, iris, pupil, lens, retina and optic nerve. Typically, light passes through cornea to iris, then pupil and is focused by lens onto retina which then converts light into electrical impulses that are carried by optic nerve to the brain. The cornea is the transparent protective layer of the eye, which is responsible for 75% of the eye's refractive power and transmits 98% of red light and 90% of blue light. It is estimated that over 10 million individuals experience corneal blindness worldwide due to diseases, age related problems, accidents, etc. Currently, corneal transplantation is the only possible method to restore vision. The success rate of corneal transplantation is 90%, but there is no/low chance of success in patients with recurrent graft failures.

The shortage of donors, the risk of infections and rejection rates made researchers to find an alternative method. To this end, tissue engineering has become an alternative remedial method which involves regeneration of bio-artificial tissues *in vitro* by culturing cells of patients or healthy donors on a biomaterial scaffold in presence of bioactive growth factors. So far, tissue engineered skin have been successfully developed and commercialized. Similarly, a tissue engineered cornea replacement could provide significant benefits over shortage of donors for corneal transplantation. However, the two major challenges to the field of tissue engineering in constructing a cornea are: transparency and tissue strength. The transparency of cornea depends on protein expression and tissue structure. The transparency of cornea is also based on the arrangement of collagen fibres and the refractive index matching of these fibrils by interstitial proteoglycans. For visible light waves to pass through the cornea, the thickness of stroma and the arrangement of collagen fibres matters. The challenges in creating tissue engineered cornea also include creating a structure that is bio-compatible and bio – resorbable (Shah et al., 2007).

There are a variety of materials being tested as corneal scaffold; the recent addition of silk fibroin to this list therefore requires careful consideration. Silk is a noteworthy protein biopolymer that is synthesized in the epithelial cells of specialized glands, secreted into the lumen and spun into fibres by the members of the classes Arachnida and Insecta, which includes silkworms, spiders, mites and fleas for cocoon formation, web formation, safety lines and egg protection; however, *Bombyx mori* silkworm derived fibroin has been widely described to date. One account of the story goes that, sericulture and the weaving of silk cloth was introduced by a Chinese Emperor who was fascinated by the silk fibres and started sericulture about 3000 BC. It is said that the Chinese managed to keep silk a secret for over 3000 years from the rest of the world. Another historical evidence suggests that sericulture is an ancient industry in India dating back to second century BC, and some historians claim Kanishka kings exported silk to Roman world during 58 BC. Nevertheless, with time, silk became an integral part of cultural identity of many communities and an integral part of daily life.

The journey of silk as a biomedical material (suture material) began in the 19thcentury because of its robust track record for non-toxicity, slow biodegradability, processing features and excellent mechanical properties. Due to silk fibroin's non-immunogenic response upon *in vivo* implantation, excellent mechanical properties, tuneable material degradation rates, it has become a suitable candidate in biomaterial selection for tissue engineering and regenerative medicine applications (Chung et al 2015). Additionally, the degummed fibres can be solubilised and dialysed to produce aqueous solutions of fibroin, which later can be fabricated into a variety of different materials viz. electro spun nanofibrous matrices, freeze-dried porous sponges, solvent cast films, micro/ nano particles, etc. and have been explored in engineering a variety of tissues. However, its use in the field of corneal tissue engineering is very limited as evident from literature reports in scientific indexing websites. A quick search in web of knowledge website using "silk fibroin" and "corneal tissue engineering" displayed 47 results, with only 1 report from India. Further, irrespective of tissue of choice, there was no study till date to investigate process dependant variations in silk biomaterials. Here, for the first time, we aim to develop silk fibroin films for potential applications in corneal tissue engineering, and in particular to provide insights into fabrication and post-fabrication dependant variations in morpho-topological, physico-chemical, optical and biodegradation properties of RSF films and cytocompatibility with model corneal cells *in vitro*.

1.2 Review of literature

1.2.1 Silk fibroin

1.2.1.1 Sources of silk fibroin

Silks, which are popular as a luxurious textile, are a class of extracorporeal fibrous biopolymers that are secreted by a variety of insects and worms belonging to animal kingdom for various physiological demands. Several species such as raspy cricket, hornets, weaver ants, bull dog ants, honey bee, bumble bee, moon moth, cashew caterpillar, mango caterpillar, may fly, silver fish, thrips, leaf hopper, etc. were found to produce silk. Typically, silkworms produce silk for metamorphosis, raspy crickets to form nests, honeybee and bumble bee produce to strengthen wax cells for laying pupae, and weaver ants produce silk to make nest by sticking many leaves together. Spider mites and pseudo scorpions were also known to produce silks. Fan mussel is a sea animal which also produces silk to stick into rocks, carp a freshwater fish also produces silk for laying eggs and attaching eggs to rocks respectively.

However, classically, silks derived from silkworms such as *Bombyx mori* and orb-spiders such as those related to *Arachnida*: *Araneidae* have been widely explored in textile industry as well as a new generation biomaterial in the field of tissue engineering and regenerative medicine. The orb-spider silk is typically composed of a core, a spidroin-like protein, a lipid coat and glycoprotein (Li *et al*., 2015). Such a heterogeneous nature of spider silk along with the cannibalistic nature of its processing, the commercial production of spider silk is restricted. In contrast, the silk fibres from silkworms are made of pure fibroin protein in the form of microfilaments that are coated with glue like protein called sericin which easily gets removed by mild boiling (Li *et al*., 2015). Apart from obtaining pure form of silk fibroin with ease of processing, the abundant availability across various parts of the globe and cost-effectiveness nature, the silk fibroin from silkworm are highly explored in various biomedical engineering applications.

Typically, the silk derived from domesticated *Bombyx mori* silkworm cocoons are widely used; however, the silks from as other wild varieties such as *Antheraea assama*, *Anthearae pernyi*, *Samia cynthia ricini,* etc. are also gaining lot of attention (Figure 1a). Lately, with the advent of genomics and cloning technologies, the silk fibroin gene was cloned into hosts such as *Escherichia coli* for mass scale production of recombinant silk fibroin protein for biomedical applications (Figure 1b).

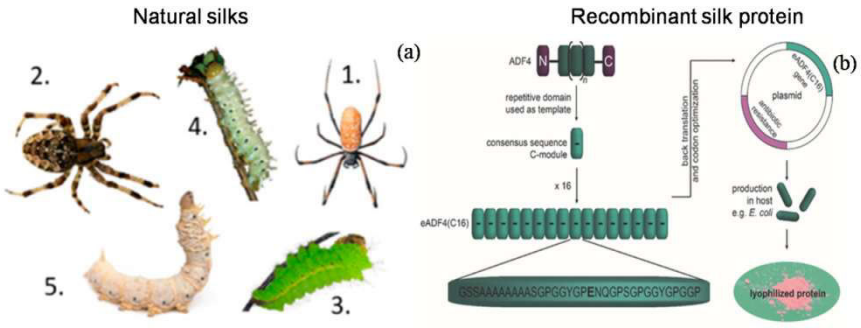

Figure 1. Various sources of silks: (a) Silks are classically obtained from various spiders such as (1) *Nephila clavipes* and (2) *Araneus diadematus* and silkworms such as (3) *Antheraea pernyi*, (4) *Samia cynthia ricini* and (5) *Bombyx mori.*(b) Recently, silk through recombinant DNA technology is also been introduced. (Reproduced from Nguyen et al 2019, © 2019 by the authors, licensee MDPI, Basel, Switzerland, and with permission from Aigner et al 2018, © 2018 WILEY-VCH Verlag GmbH & Co. KGaA, Weinheim).

1.2.1.2 Structure and composition of silk fibroin

Silk from *B. mori* is composed of two types of proteins, the main being silk fibroin in the form of a water-insoluble filaments that are joined by another gummy layer of protein called sericin. Through a process called degumming involving mild boiling in a detergent solution, sericin is washed-out (Koh et al 2015). Silk fibroin from *B. mori* consist of three protein subunits viz. heavy chain of about 350 KDa, light chain of about 26 KDa and a glycoprotein P25 of about 30 KDa (Mondal et al 2006). Inoue et al., 2000 found that H-chain, L-chain and P25 subunits are assembled in a molecular ratio of 6:6:1 both in cocoon as well as in the silk fibroin protein within the posterior gland of the silkworm. The design feature of silk domain includes N- terminal and C- terminal peptide domains including highly repetitive sequences in between. The N terminus chain contains 130 amino acids and C terminus chain contains around 100 amino acids (Ebrahimi 2015). The central core of silk fibroin sequence is composed of twelve highly repetitive hydrophobic regions ,made up of amino acids such as Gly-Ala-Gly-Ala-Gly-Ser/Tyr (GAGAGS/Y) and GAAS tetramers at the terminus, and eleven interspersed amorphous regions rich in Gly. Disulphide and hydrogen bond network within the core fibroin sequence leads to the formation of a stable highly organized anti-parallel β-sheet crystalline structures (Ma et al 2002). The interspersed amorphous domains involve hydrogen bonding and leads to the formation random coils and α-helical structures (Keten et al 2010). The silk fibroin has two crystal structures: silk I - a metastable structure with crank or S zigzag structure and silk II

- an anti-parallel β-sheet structure. Silk fibroin when in solution form was reported to exhibit silk III structure at the air/water interface.

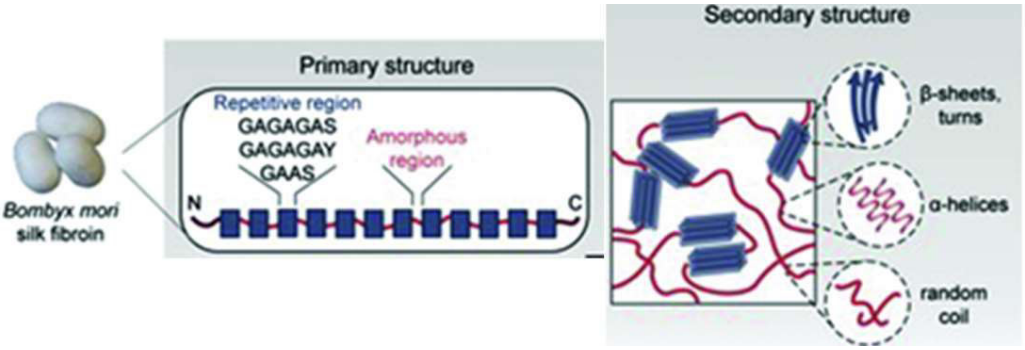

Figure 2. Structural features of silkworm silk fibroin: Primary sequence includes N and C- terminal units with 12 repetitive and 11 amorphous regions in-between. These units interact by hydrogen and disulphide bonds to form random coils, alpha helices and beta sheets in their secondary structure (Reproduced with permission from Mc Gill et al 2019, © 2018 WILEY-VCH Verlag GmbH & Co. KGaA, Weinheim).

1.2.2 Silk fibroin in tissue engineering

1.2.2.1 Fundamentals of tissue engineering

With the developments in the field of materials science and cell/ developmental biology a new discipline termed as tissue engineering has evolved. Langer and Vacanti 1993 defined tissue engineering as *"an interdisciplinary field that applies the principles of engineering and life sciences toward the development of biological substitutes that restore, maintain, or improve tissue function or a whole organ"*. The most common application of tissue engineering is the replacement/ reconstruction or regeneration of damaged tissues/ organs that are lost due to disease, accident and ageing. Typically, it refers to the practice of conjoining a triad of cells, biomaterial scaffolds and bio-active cues to develop bio-artificial tissue substitutes. Typically, cells from autologous origin are preferred, however, cells from allogenic origin including those induced pluripotent stem cells are also under investigation. Scaffolds are made from a variety of materials viz. metals, polymers, ceramics, and composites, in various forms viz. fibrous mats, porous sponges, hydrogels, films, particles, etc. Bio-active cues involve growth factors, anti-inflammatory molecules, pro - angiogenic peptides, etc. either in soluble form or in immobilized form along with scaffold. Apart from these three components, bioreactors have also been widely explored in the field to offer automated, reproducible and controlled environmental factors that could improve the quality of engineered tissues at relatively reduce production costs

(Martin et al. 2004). However, amongst the three, the biomaterial scaffold is the critical component that determines the fate of the entire process. The scaffold typically fills the tissue void, provides structural support and acts as a reservoir for growth factors and/or cells that have the ability to reconstruct the damaged tissue within the body upon transplantation.

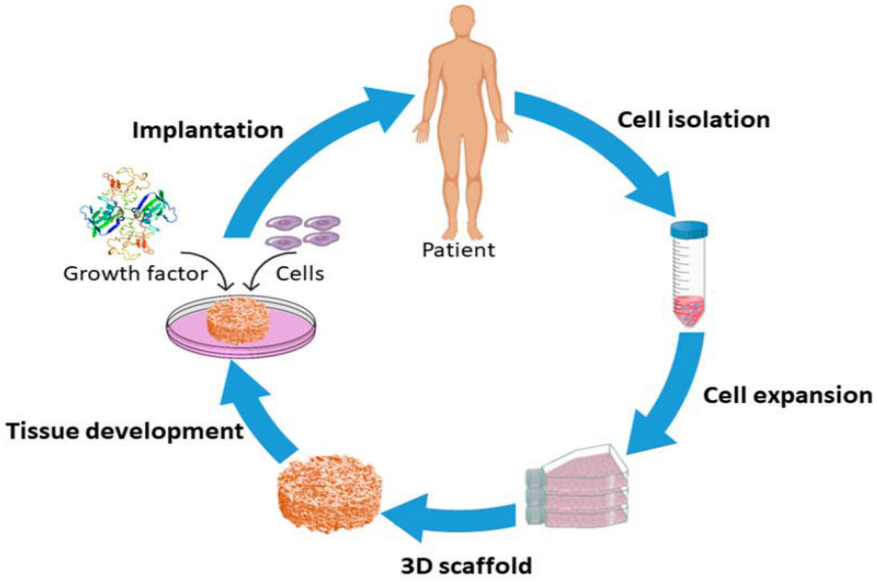

Figure 3. Schematic of tissue engineering process: Typical tissue engineering process involves isolation and expansion of cells from a patient, culture in 3D scaffold to develop into a mature tissue in presence of various growth factors and subsequently implantation into the patient (Reproduced from Asadian et al. 2020, © 2020 by the authors. Licensee MDPI, Basel, Switzerland).

1.2.2.2 Silk fibroin as a scaffolding biomaterial

An ideal scaffold for tissue engineering applications typically requires the following features (Li et al 2013): (a) *Architecture:* pore size, pore density, pore inter-connectivity are critical parameters to consider while designing a scaffold. They should be optimized to allow cellular infiltration, exchange of nutrients and wastes, and diffusion of gases throughout scaffold so as to generate a viable tissue without any necrotic core. (b) *Biocompatibility:* since the material is intended for use in clinical applications, the material would invariably come in contact with blood and tissues. Therefore, it is important to design the scaffold in a way that it evades immunological reactions and offers attractive biocompatibility. (c) *Bioresorbability:* the scaffold is a typically designed as a temporary supporting structure and it is anticipated that the scaffold should degrade over time and leave space for native tissue growth. The scaffold degradation properties should be tuned

to match the native tissue regeneration rate. (d) *Mechano-biology:* cell to native extracellular matrix (ECM) interactions are typically reciprocal and often are mechanically remodelled by the cells to aid in cell migration, proliferation and differentiation. The scaffold intended for tissue engineering applications should also be designed to mimic the native ECM features. (e) *Bioactivity:* although the concept of biomaterial scaffold in tissue engineering was introduced with a note of biomaterial being bio-inert, several developments in the field have recognized the importance of modifying the biomaterial to be a bio-active in order to achieve desirable cellular response. Therefore, it is important to design a scaffold by imparting bio-active cues such as growth factors – pro - angiogenic factors, etc. to achieve desirable tissue features.

Figure 4. Features of silk fibroin as a biomaterial: availability, processability, biocompatibility, biodegradability, attractive physico-chemical and other properties are some of the characteristic features of silk fibroin as a biomaterial.

There are several biomaterials like natural polymers, synthetic polymers or a combination to provide a structural and functional framework, which mimics the features of native ECM. Amongst them, silk fibroin was found to be favourite biomaterial for scaffolding in tissue engineering. Surgeons started using silk as a suture material from 19thcentury onwards. This marked the new beginning of silk from being a textile material to a biomaterial in the field of biomedical engineering. In the search for new materials as scaffolds for supporting cell growth, proliferation and differentiation, several researchers in the field of tissue engineering and regenerative medicine got attracted towards silk, majorly due to abundant availability, successful history of its use a suture material, outstanding biocompatibility, tunable mechanical properties, versatile processing and modification methods(Figure 4).The properties of silk make them distinguishable from all

other natural materials known to date, and considering the remarkable physico-chemical properties of silk fibroin, United State Food and Drug Administration approved silk as a biomaterial for some medical devices (Huang et al., 2014).

Availability, affordability and processability: A variety of biomaterials are being investigated for various biomaterial applications. However, relatively production and manufacturing of biomaterials in large scale requires huge investment of money, time and labour. In contrast, silk production is an age-old practice done on a massive scale. According to the data provided by Ministry of Textile, India, about 27.24 million metric tons of silk is produced per year through sericulture process across various states of India for textile industry. In India, majority of the silk is produced in five states such as Karnataka, Andhra Pradesh, Tamilnadu, West Bengal, and Jammu and Kasmir. Besides, its production cost is relatively cheap than any other known biomaterial so far. Moreover, silk is available around the year and transported and shipped at ambient conditions. One of the major advantages using silk in the field of tissue engineering is the ease of processing. Silk fibroin inherently comes in the purest form as a fibre, typically coated with gummy-like protein called sericin and can be easily washed away by treatment in sodium carbonate solution. The silk fibres can be used as such for biomedical applications or can even be reconstituted into aqueous silk solution involving lithium bromide. With such extraordinary availability, affordability and processability, silk fibroin stands out from any other biomaterial for biomedical applications.

Physico-chemical and other properties: The striking equilibrium of breaking strength, modulus, toughness, and elongation makes silk different from other biomaterials known-till date in its mechanical properties. The mechanical property of silk depends on the process parameters, molecular structure, supra molecular structure, climate and ambience. Nguyen *et al* 2019 reports that the tensile strength of silk is greater than poly L-lactic acid and collagen. The mechanical properties affect cell migration, cell differentiation and morphology. The strong interactions between the nano fibrils in the threads and the fine channels in the thread helps in dispersing energy. Hakimi *et al* reports that the brittle nature of *B. mori* silk is due to the higher crystalline regions containing poly-Gly-Ala β sheets. Thermal stability of silk even at 200 °C makes it a useful biomaterial in the field of optoelectronics (Nguyen et al., 2019). SF has been approved by US FDA in 1993 for using it as a suture (Altman et al 2003). The scaffolds are the link of cells and growth factors. A scaffold with less immunogenicity, less degradation etc is the

best one and here SF satisfy all these functional requirements- cell growth and growth factors (Li et al 2013). Further, optical clarity of silk fibroin films makes it one of the attractive biomaterials for applications such as corneal tissue engineering and other bio-functional optical interfaces.

Biocompatibility: The silk fibroin from *B. mori* has been domesticated by human over centuries and has proved as one of the best and effective biomaterials. The biocompatibility of silk fibroin has found its position in the field of biomedical. However, it is reported as a clinically approved biomaterial for human use. It was found that sericin- the outer coating of silk could cause allergic reaction, immunogenicity, and the release of inflammatory marker, which raised concerns about biocompatibility of silk fibroin. However, the raised concerns were solved once sericin is extracted from silk fibroin. The degumming is the process of extraction of sericin; once the degumming is done, it was found that fibroin could support cell proliferation and attachment of various cell types. Silk fibroin films shows biocompatibility to human mesenchymal stem cells in-vitro and shows more proliferation than collagen-based scaffold. Silk fibroin coated membranes shows better adherence and proliferation of fibroblasts (Hakimi *et al*., 2006). The silk based materials provides appropriate biological environments for cell adhesion, differentiation and the ease to process the silk protein into a variety of material morphologies and their low toxicity and immunogenicity proves that silk is an interesting and effective biocompatible material (Eagana & Scheibel, 2010).

Biodegradation: Biodegradation is one of the essential properties for a substitute biomaterial. Biodegradation can be defined in such a way that the scaffold should ideally degrade at a similar rate to the growth of new tissue, which in turn helps the engineered tissue to get integrated into the surrounding host tissue (Kearns *et al*., 2008). The recognition sites for proteolytic enzyme, matrix material and morphology determine the rates of biodegradation. Huang et al 2004 reports that Protease XXI can degrade silk films by altering strength and surface roughness over 17 days. Hakimi *et al*. 2006 reports that there is steady absorption of silk fibres over long periods *in vivo*. The rate of absorption is directly depending on the mechanical environment, implantation site, type of silk, the secondary structure and diameter of the silk (Ngyuen et al., 2019). As the degradation of protein based scaffolds results in the formation of amino acids that are easily assimilated by cells, without any other known adverse reactions, silk fibroin presents diverse benefits for biomedical applications as compared to other synthetic or natural polymers (O' Brien,

2011). The unique processability of silk fibroin into biomaterials with different crystalline to amorphous structure ratio enables to fine tune the biodegradability as per user requirements.

1.2.2.3 Silk fibroin in various tissue engineering applications

Silk fibroin has been selected as a good candidate biomaterial and has been extensively using in various tissue engineering fields owing to its impressive mechanical strength, hierarchical structure and other diverse range of attractive properties. To date, it has been explored in engineering various hard tissues such as bone, etc., soft tissues such as liver, skin, etc., and other specialized tissues such as pancreas, ovarian tissue, etc. (Figure 5).

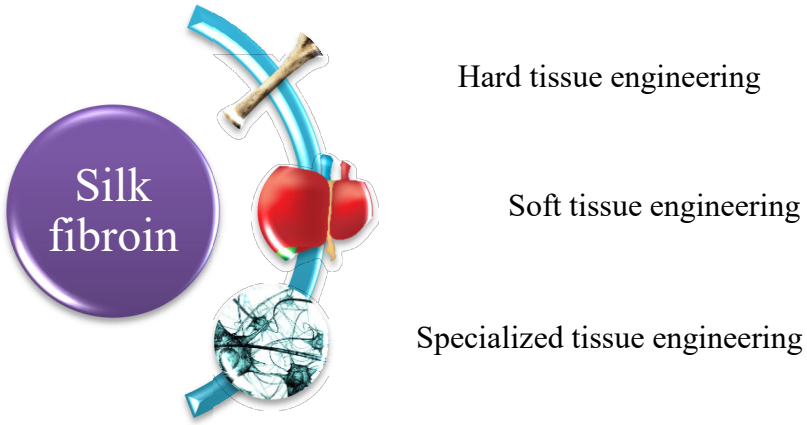

Figure 5. Schematic of silk fibroin in various classes of tissue engineering: silk fibroin has been reported to be used as a scaffolding biomaterial for hard tissues such as bone, teeth and soft tissues such as liver, tendons and ligaments and specialized tissues such a nerve, ovary etc.

Hard tissue engineering: Silk fibroin has been used as a biomaterial in bone tissue engineering in various forms. Besides using native *B. mori* silk fibroin, the combination of it with others such as hydroxyl apatite are also used to a wide extend for bone regeneration. Tanaka et al 1999 showed that the nano hydroxyl apatite - silk fibroin sheets were compatible and support effective adhesion and proliferation with bone marrow derived mesenchymal stem cells (MSCs).It was also found to support osteogenic differentiation of human MSCs (Kasoju et al 2012, Meinel et al 2006). Melke et al 2016 done an invivo study on rats using collagen and porous silk scaffold for bone regeneration and found that porous SF scaffolds exhibit architectures with hierarchical organization which is comparable to cortical and trabecular bones and can facilitate osteogenesis within the defect site. They also found that porous silk scaffold was similar to ECM of osteoblasts.

Similarly, several other studies used silk fibroin as a scaffolding material for bone tissue engineering applications. Another hard tissue of interest is tooth which is a complex construct with 4 dental tissues such as enamel, dentin, cementum and pulp. Silk fibroin has been explored in dental tissue engineering as well. For instance, Galler et al 2011 has demonstrated successful isolation of postnatal stem cells from various oral cavity parts and grown on silk scaffolds. They found successful replacement and regeneration of damaged teeth. Xu et al 2008 also examined silk scaffolds for dental tissue engineering by seeding postnatal rat tooth bud cells and found bioengineered tissue simultaneously supporting osteo-dentin formation. Cartilage is another widely explored tissue. It is an avascular connective tissue with limited ability for self-repair. Cai et al 2002reported that the silk fibroin coated with polylactic acid improved attachment and proliferation of osteoblasts. Silk fibroin has also been blended with other materials such as chitosan, collagen, poly (L-lactic acid), agarose, cellulose, hyaluronic acid, etc, for cartilage tissue engineering.

Soft tissue engineering: Skin is the largest organ in the human body. Silk fibroin-based tissue engineering approaches are being attempted to find an alternative for skin repair/ replacement. Min et al 2004 demonstrated fabrication of silk fibroin electrospun nano-fibrous scaffold, evaluated its interaction with keratinocytes and fibroblasts and found excellent cytocompatibility. SF scaffolds cross-linked with formic acid upon long term co-culture with fibroblasts and keratinocytes resulted in fabrication of metabolically active and functional dermal-epithelial equivalents (Dal et al 2006). SF thereby is a good choice for wound healing and repair. Liver is the largest internal organ in the body and hepatic tissue engineering has emerged as an alternative treatment approach to manage liver repair and reconstruction. Gotoh et al 2004, 2011 prepared SF conjugated with lactose cyanuric chloride and evaluated hepatocyte response. They found that the engineered hepatic tissue exhibited liver specific functions and 8-fold increase in cell attachment to that of unconjugated ones. Cirillo et al 2004reported the fabrication of SF films and successfully showed cell adhesion and function of rat liver cells on SF films. Kasoju et al 2012 reported a silk fibroin and galactosylated chitosan based electro spun nanofibrous scaffold that mimic composition and structure of native ECM and showed successful application in hepatic tissue engineering. Ligaments and tendons are dense connective tissues that facilitate normal joint movements. They are the ones which hold the bones tightly at the joints. Silk fibroin has also proven to be effective in attachment and proliferation of ligament cells. For instance, Chen et al 2003 evaluated silk fibroin coated

with Arg-Gly-Asp for ligament interface healing and found effective cell adhesion, growth and collagen matrix production.

Specialised tissue engineering: There are quite a few specialized tissues in our body such as nerve tissues, pancreas, ovaries, etc. Nervous system is a biological network broadly classified into peripheral and central nervous system. Tissue engineering strategies for peripheral nervous system are focused on developing a nerve graft that would aid in regeneration of nerve cells (Schmidt et al 2003). Ren et al 2009 fabricated SF scaffolds coated with hyaluronic acid and found high affinity to neural cells. Madduri et al 2010 developed SF nerve channel with glial cells and nerve growth factors and reported axo-glial outgrowth from the explants. Lately, Das et al 2015 described the preparation of gold nanoparticle embedded silk fibroin-based nerve guidance conduit and successfully showed its efficacy in repairing a neurotmesis grade sciatic nerve injury in rats. Eardrum (tympanic membrane) is another interesting specialized tissue present inside ear that has the ability to aid in hearing. SF based TE studies have been reported to develop bio-artificial eardrum tissues (Levin et al 2009). For examples, Levin et al 2010 evaluated potentiality of SF as an alternative graft for myringoplasty surgery and found enhanced cell adhesion, attachment and proliferation of human tympanic membrane keratinocytes. Pancreas is yet another specialized tissue with endocrine and exocrine functions in the body. SF has also been recently explored in pancreatic tissue engineering. For instance, Kumar et al 2018 evaluated hepatocyte encapsulated silk hydrogels for hepatic tissue engineering. They found that silk hydrogels provide a suitable environment for islets and enable good islet viability and functionality and hence a best material for hepatic tissue engineering strategies.

1.2.3 Silk fibroin in corneal tissue engineering

1.2.3.1 Corneal anatomy and physiology

The outer layer of the eye is called cornea, which is a transparent avascular connective tissue, which acts as the primary structural barrier of the eye, which is relatively simple structure and is composed of three different tissues: epithelium, stroma and endothelium, measuring approximately 11.5 to 12 mm in diameter. It is 0.5 mm thick at the centre and the thickness increases towards the edges (Figure 6) (DelMonte et al., 2011). The corneal shape and curvature is determined by biomechanical structure and extrinsic environment governs. The corneal epithelium consists of different layers of stratified squamous epithelium, which resides anterior to Bowman's layer. A mesenchymal cell type called

keratocyte populates the corneal stroma. Innermost layer of endothelial cells, which resides in a posterior fashion, is known as Descemet's membrane.

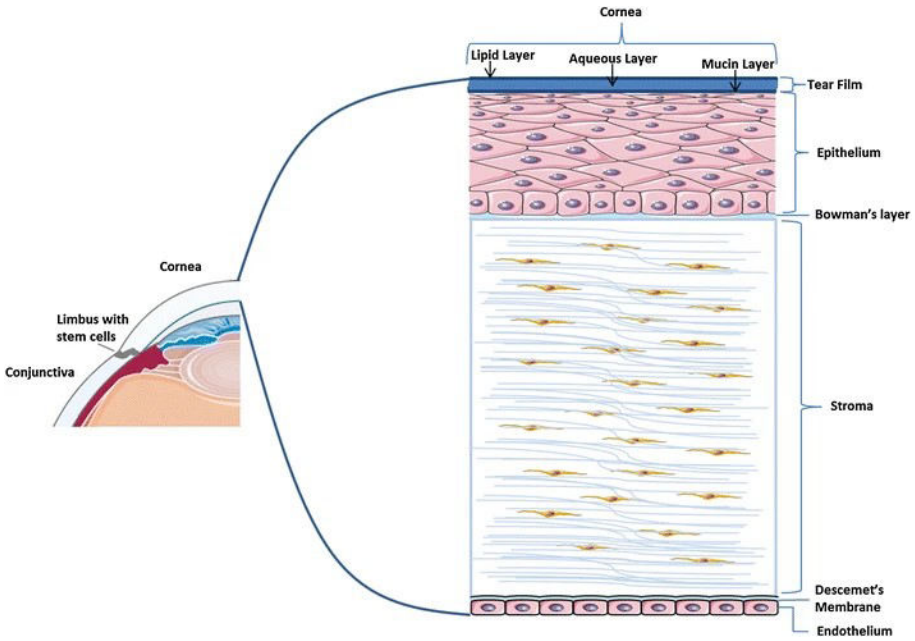

Figure 6. Anatomy of eye and representation of corneal anatomy: The figure Shows different cell types of woven fibril mat, lamellae and hexagonal lattices on endothelium which are present on the cornel layers (Reproduced from Rowsey and Karamichos 2017, © The Author(s) 2017).

Epithelium: Epithelium is the outermost layer of cornea which is responsible for the refractive power of eye and also protects the eye from microbial attack and other external environmental factors. Epithelial layer is developed from the ectodermal layer during the development and upon maturation it is typically stratified by non-keratinocyte squamous cells with perfect uniformity. This squamous epithelium comprises of 5-6 cellular layers that are covered by tear film (Farjo et al 2008). Corneal epithelial layer has7-10 days of lifespan and endure programmed cell death (Hanna et al 1961). The epithelial structure is highly organized, which consists of superficial, wing cells and basal cells. The superficial cells form a mean of 2 to 3 layers of flat polygonal cells. Basal layer of cornea contains columnar epithelial cells of about 20 µm height (Wiley et al 1991). Just anterior to the basal layer of cells and beneath the superficial cells are the wing cells. Epithelial basement membrane has a thickness of 0.05 µm thickness with type IV collagen and laminin from basal cells.

Bowman layer: It is an acellular, non-regenerating layer between the epithelial basement membrane and the anterior corneal stroma. Stroma is approximately 8 to 15 µm

thick in humans and it is composed of randomly arranged fine collagen fibres and proteoglycans within an ECM. It is in the anterior portion of stroma and is not a true membrane. Epithelial innervation happens when unmyelinated nerve axons penetrate this layer irregularly. This smooth layer helps the cornea to maintain its shape. However, if disrupted, it will not regenerate and leaves a scar (Sridhar et al., 2017). Lagali *et al*. 2009 demonstrated that this layer might act as barrier to protect nerve plexus as well as to prevent direct traumatic stromal damage.

Stroma: The corneal stroma provides structural framework to the cornea. The stroma is characteristically transparent, and it is the result of precise organization of extracellular matrix and stromal fibres Stroma comprises about 90% of total corneal thickness and is thicker at the periphery and thinner to the centre. These fibrils are packed in parallel-arranged layers or lamellae and the stroma contains 200 to 250 distinct lamellas; each layer arranged at right angles relative to fibres in adjacent lamellae. Stroma is also responsible for the mechanical integrity and more importantly for the transparency of the cornea (Boote et al 2010). Stroma is composed of type I and type V collagen fibres in a highly organized manner (Wilson et al 1996). These structures are covered by proteoglycans with keratin sulphate/chondroitin sulphate. Deeper layers are more organized than superficial layers (Mobaraki et al 2019). The major cell present in the stroma is keratocytes which are able to synthesise collagen and glycosaminoglycans for stromal homeostasis (Jester et al 2010).

*Descemet's membrane :*It is a basement membrane of the corneal endothelium and measures about 3μm in thickness in children and about 10 μm in adult humans. Endothelial cells are responsible for the formation of Descemet membrane and it is rich in glycoprotein. The Descemet's membrane is a structure made up of Type IV and Type VIII collagen, laminin and fibronectin. This membrane is elastic, but the exposure to shearing stress can result in tear. Descemet folding's resulted from the asymmetric swelling of the posterior stroma and structural restriction imposed by the limbus (Eghrari *et al*. 2015).

Endothelium: Endothelium is a monolayer with cuboidal cells which seems like a honey comb structure (Beebe et al 2010).. It contains a large nucleus and abundant cytoplasmic organelles. The presence of cytoplasmic organelles suggest cells are metabolically active and secretory. Endothelial layer maintains cornea in a dehydrated state (78% water content). Over time, cells get flattened with a homogenous acellular layer and become Descemet's membrane (Watsky et al 1989). These flattened cells become 4 μm

thick in adults. They also possess gap and tight junctions with sodium potassium ATP ase pumps. This passive bulk fluid movement is fuelled by the process of transporting ions to generate the osmotic gradient. The damage to these cells can increase the influx of water to the stroma. An increase in variation of cell shape and an increase in cell size correlate to the reduced ability of the endothelial cells to deturgesce the cornea (Stiemke et al 1991). Cell density of human endothelial layer at birth is 3500 cells/mm^2 and decreases by 0.6 % per year (Polse et al 2010). The damage to these cells can increase the influx of water to the stroma. The number of endothelial cells decreases with age, but the existing cells have capacity to stretch and take up the left space and grow in size. They also lose their hexagonal shape.

1.2.3.2 Corneal tissue engineering and regenerative medicine

Being the outermost layer of eye exposed to various environmental factors including heat, hazardous chemicals, pollutants and pathogens, cornea is highly vulnerable to damage (Sommer 1982). According to World Health Organization, about 2.2 billion people have some sort of vision impairment, of which 1 billion people suffer from moderate to severe distance vision. According to the National Programme for Control of Blindness (NPCB), India statistics, about 6.8 million people suffer from vision impairment of which about 120,000 are related to corneal blindness (Gupta et al 2013). Currently, corneal transplantation is offered as a treatment for corneal damages wherein the damaged corneal tissues are replaced with donor corneal tissue form a healthy volunteer. Unfortunately, shortage of donors is a major bottleneck in eradicating corneal blindness (Whitcher et al 2001). Corneal tissue engineering is becoming an attractive therapeutic alternative towards corneal regeneration and reconstruction. Various researchers have attempted to engineer corneal layers such as epithelium and endothelium through cell sheet engineering (figure 7) approach and stroma reconstruction through biomaterial based strategies (Umemoto 2013).Different biomaterials are being tested *in vitro*, *in vivo* as well as in clinical studies, however, the loss of transparency and lack of strength are some of the bottlenecks in clinical success (Peh et al 2011). Efforts are on across the globe in finding effective biomaterial solutions for clinically compliant corneal equivalents.

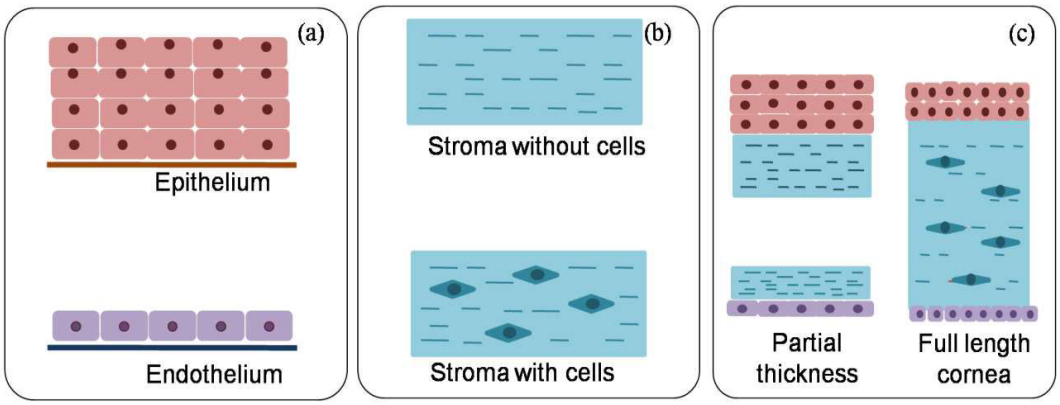

Figure 7. Corneal tissue engineering approaches: (a) corneal epithelial and endothelial tissues can be generated by scaffold-free cell sheet engineering, (b) stromal tissue with or without cells as well as (c) partial and full thickness corneal tissues can be generated by scaffold-based top-down or bottom-up tissue engineering methods.

1.2.3.3 Silk fibroin as a biomaterial in corneal regeneration

A quick search in web of knowledge website using "silk fibroin" and "corneal tissue engineering" displayed 47 results. Single digit number of publications per year (Figure 8a) shows that this particular field is not yet explored to its full extent and therefore clearly indicates potential research gap. Further, when the publications were sorted as per country wise, China topped the list with 13 publications followed by USA - 12, Australia - 10, South Korea - 7 and Germany - 3 (Figure 8b). Some of the notable contributions in the field are mentioned here. Madden et al 2011 prepared silk-based film with collagen coating on its surface to assess the differentiation and proliferation of corneal cells. It was found that the cell attained maximal confluence and became an effective substrate for keratinoplasty. In the field of ocular drug delivery, Dong et al produced silk film coated liposomes containing ibuprofen and showed promising delivery of drugs to the ocular surface (Dong et al 2015). Applegate et al. published a report on silk fibroin hydrogel preparation by photo-crosslinking using FMN and subsequent application in corneal bioengineering (Applegate et al 2016).

Zhou *et al* 2019 investigated the application of PVA/SF/n-HA composite hydrogels in the field of artificial cornea tissue engineering and reported that, adhesion and reproduction of cells of human eye fibroblasts on composite hydrogel cross-linked with different GP content was found high and favourable. Wang *et al* 2017 reported the development of innervated silk based corneal tissue models, which supports dense and

long neuronal innervation with aligned hCSSCs for the stromal layer and multilayer hCEcs for the epithelium. J E Song *et al* a ,b 2018 studied, the application of silk fibroin-glycerol blend films for corneal transplantation purpose and reports that, blending of glycerol led to the formation of elastic structures without cracks and with less microns of thickness as compared to silk fibroin films. *In vitro* study using, rCEnCs demonstrated that glycerol does not affect its viability and activity.

Out of 47 results, only 1 is from India, therefore, there is tremendous potential for silk based corneal tissue engineering research in India. Ramachandran et al 2020 recently published a detailed study on the development, characterization, and *in vitro* evaluation of different varieties of silk substrate for corneal endothelium culture. The study explored the use of silk fibroin from non-mulberry varieties of silk and it was reported that films made from these sources also support growth, adhesion, and function of corneal endothelial cells.

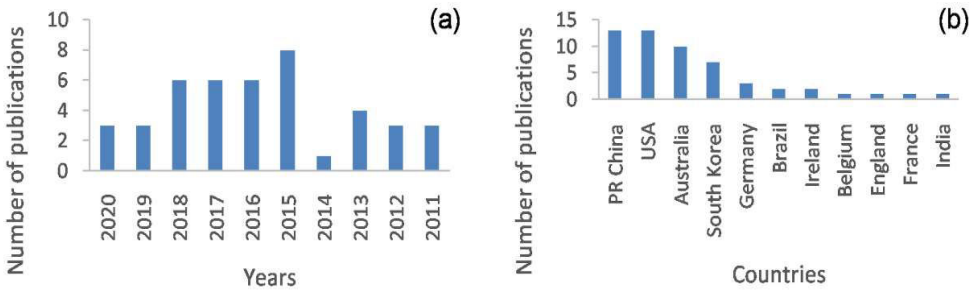

Figure 8. Web of knowledge database results: (a) number of publications per year, and (b) number of publications per country. Keywords used: "silk fibroin" and "corneal tissue engineering".

1.2.4 Process – property relationship in silk fibroin biomaterials

1.2.4.1 Pre-fabrication processing

Silk cocoons have to be processed before fabricating into scaffold form for potential applications in tissue engineering. Degumming is a process in which raw silk fibres are treated with mild detergents or other chemicals at elevated temperatures to remove the gummy outer layer i.e. sericin and thereby pure silk fibroin fibres are obtained. Type/concentration of degumming chemical/agent, duration of degumming, temperature used if any are major process parameters that could influence the efficiency of degumming as well as the quality of resultant silk fibroin fibres. For instance, Wray et al 2011 used boric acid-sodium borate buffer, sodium carbonate, urea and succinic acid as degumming

reagents and found that different reagents influenced tensile strength of resultant silk fibroin fibres differently. Further, the degumming time was also found to influence yield percentage and protein structure, wherein, they described that as the degumming time increases, the molecular weight of silk fibroin was lowered. In a similar study, Wang et al 2015 compared sodium carbonate, neutral soap and an undisclosed silk protein surfactant as degumming reagents and reported that silk protein surfactant as an environmentally friendly degumming agent. Teh et al 2010 also evaluated the effect of degumming time on SF features and found that prolonged degumming leads to reduced mechanical integrity and fibroin fibrillation. Further, in an interesting study, Tsubouchi et al 2003 investigated the effect of degumming on silk fibroin and its cellular response and demonstrated that increase in degumming time led to silk fibroin fibres that have reduced cell proliferation rate.

1.2.4.2 Fabrication processing

Silk fibroin can be fabricated into a variety of forms viz. films, hydrogels, porous sponge, micro/ nano fibrous matrices, etc. Depending on the process, the parameters involved would strongly influence the properties of resultant SF product. For instance, Tamada et al 2005 reported a new process of fabricating SF porous sponges by freeze-thaw of fibroin aqueous solution in presence of a small amount of an organic solvent. It was demonstrated that solvent type, fibroin concentration, freezing temperature and time influenced the sponge fabrication and its porosity as well as mechanical properties. In a similar study, Kasoju et al 2016 reported preparation of SF hydrogel by non-solvent induced phase separation. It was described that the concertation of non-solvent influenced the gelation time, pore properties and secondary structural content in resultant SF hydrogel. Bray *et al*., 2011 evaluated silk films for use in repairing the cornea after injury due to their transparent nature and high degree of biocompatibility. They found the excellent transmission % and transparency for silk films. SF was also explored in combination with other polymers such as agarose, collagen etc. and effect of such additives on SF products was also studied. For examples, Jin et al 2004 prepared silk and poly (ethylene oxide) (PEO) blend film. After PEO was extracted, the porosity and surface roughness of resultant silk films was enhanced. Further, addition of PEO was found to enhanced elasticity and hydrophilicity of films. Kong et al 2016 evaluated the effect of corneal cells onto electrspun silk scaffold and found that the scaffold has a high volume-to–surface area ratio and porosity, which

simulated natural ECM and provided atmosphere for corneal cells to attach, move, proliferate and differentiate.

1.2.4.3 Post-fabrication processing

Post-fabrication processes are usually done to enhance the properties of resultant silk fibroin products. Typically, they are performed to modulate the beta sheet structure of silk in the products so as to fine-tune properties such as stiffness, degradation, etc. It was reported that high beta sheet content provides high tensile strength, low degradation rate etc. For instance, Lu et al 2010 performed post-fabrication processing of silk films by methanol and water annealing and found that the methanol treatment induced more beta sheet formation and thereby reduced biodegradation of films. In a similar study, Lawrence et al 2010 investigated the effects of hydration on silk film after methanol annealing and water annealing. Also, oxygen was easily permeable in methanol annealed samples. FTIR spectra showed an increased beta sheet on water annealed samples, while methanol annealed did not change. Liu et al 2020 generated SF nanoparticles in RSF solution by autoclaving and subsequent freeze-drying and PEG annealing resulted in a new type of SF sponge with unique micro- and nanoporous structures with flexibility. The sponges obtained exhibited high-water absorption capacity (~40 times the dry weight of the sponge) and the pore size was different to that of non-annealed. Such treatments provide an option to adjust the secondary structure and crystallinity of SF materials in mild conditions, thereby controlling the properties of SF mats for specific applications (Huang et al 2014).

1.3 Research gap

As detailed in previous sections, silk fibroin from *Bombyx mori* silkworms, displays great potential value as biomaterial for tissue engineering in general and for corneal tissue reconstruction. Most of the research was carried on preparing various forms of biomaterials from silk fibroin viz. porous sponges, films, electrospun matrices, hydrogels, etc. Some of the literature was also found to be highlighting the application of silk fibroin in engineering various tissues viz. skin, bone, liver, etc. And few reported on the physical, chemical, mechanical properties and bioactivity of silk fibroin-based biomaterials. However, no study was found on understanding process-dependant variations in silk fibroin biomaterials in general, in the context of corneal tissue engineering.

1.4 Hypothesis

A tremendous amount of exploratory research was recorded in the literature in the field of silk-based biomaterials. Given its extraordinary properties as a biomaterial, ease of

processing, availability around the year and relatively less expensive nature has made it a biomaterial of choice for many in the field. Surprisingly, no study was taken up so far to investigate the process dependant variations in silk fibroin-based biomaterials in the context of corneal tissue engineering. To this end, we formulated the current study with a hypothesis that silk fibroin when processed into films, following various fabrication and post-fabrication treatments, show variations on morpho-topological, physico-chemical, optical and biological properties of RSF films in the context of corneal tissue engineering.

1.5 Aim and objectives

To this end, here we formulated the current study with an aim to fabricate *B. mori* silk fibroin films and to investigate whether or not the processing parameters show any variations on its morpho-topological, physico-chemical, optical and biological properties. For this purpose, we have set the following objectives:

a) To collect and degum *Bombyx mori* silk cocoons into silk fibroin fibres and characterized its morphological and chemical/structural properties.

b) To reconstitute the degummed fibres into aqueous silk fibroin solution and characterize its molecular weight and chemical/structural properties.

c) To process RSF solution in AQ, FA and HFIP into films by solvent casting approach, followed by annealing with methanol, water and steam, and to characterize its morphological properties (SEM, surface roughness), physical properties (contact angle, swelling index, water uptake, water vapour transmission%),chemical/structural properties (FTIR),optical properties (optical clarity, absorbance spectra and transmission% in UV-Visible range), degradation properties.

d) Finally, to evaluate its cytotoxicity with L929 cells and cytocompatibility with SIRC cells to determine its potential application in corneal tissue engineering.

Chapter 2: Materials and Methods

2.1 Materials

Domesticated *Bombyx mori* silk cocoons were purchased from a local farmer based in Palakkad, Kerala, India. Lithium bromide, Sodium carbonate, Formic acid (≥ 96%), Sodium azide, Sodium dodecyl sulphate, Acrylamide, Ammonium per sulphate, N,N'-methylene bisacrylamide, Tris buffer, Dialysis bag (molecular weight cut-off 12-14 KDa), Sodium hydroxide, Paraformaldehyde and Protease (type XIV from *Streptomyces griseus*, ≥3.5 units/mg) were purchased from Sigma-Aldrich, India. 1,1,1,3,3,3-Hexafluro-2-isopropanol (HFIP, 98%), N, N,N',N'-Tetramethylethane-1,2-diamine and Methanol were purchased from Spectrochem, India. Glycine, Alamar blue, Hoechst, Phalloidin - rhodamine and Loading dye were purchased from Invitrogen Thermofisher, India. Protein ladder and MTT reagent was purchased from HiMedia, India. Coomassie brilliant blue R250 was purchased from TCI, India. Phosphate buffered saline tablets were obtained from Takara, India. Hydrochloric acid, Isopropanol and Acetic acid were procured from Merck, India. Dulbecco's Modified Eagle's medium (DMEM), Fetal bovine serum (FBS), Penicillin streptomycin (100X), Trypsin were bought from Gibco, India. L929 cells from American Type Culture Collection, USA. Triton X 100 was purchased from Promega corporation, MB Grade, US.

2.2 Preparation and characterization of degummed silk fibroin (DSF)

2.2.1 Preparation of DSF

Degumming is a process performed to remove gum-like sericin coating along with other contaminants such as calcium oxalate crystals from silk fibres and thereby to obtain pure silk fibroin fibres (Figure 9) (Rockwood et al. 2011). Firstly, exterior fibrous material that might contain dirt and other environmental contaminants on the surface of cocoons was manually removed. The cocoons were cut at one end and then the pupa was removed using forceps. The pupae were discarded as per biological waste disposal guidelines of BMT Wing, SCTIMST, Trivandrum, India. The cocoons were then cut into small pieces of size about 1cm^2 with fine scissors. A glass beaker containing 2 L of distilled water was kept for boiling; it was covered with aluminium foil to restrict evaporation. Measure 4.24 g of sodium carbonate and slowly add to the boiling water (this gives a solution of 0.02 M solution). Subsequently, add 5 g of cut cocoon pieces to it and keep boiling for 30 minutes. Occasionally stir with a spatula for good dispersion of cocoons. The degummed fibres were then collected using a glass rod and thoroughly rinsed with distilled water to get rid of residual salt. The spent sodium carbonate solution was discarded once it comes to room

temperature. The degummed fibres were spread on an aluminium foil and kept for drying in hot air oven (LabCare, India) overnight. The weight of degummed fibres was recorded, and the yield percentage was calculated using *Equation* (1).

$$Degummingyield\ \% = \frac{Wei\quad of\ degummed\ fibers}{Weigh\ \ of\ raw\ fibers} \times 100 \qquad Equation\ (1)$$

2.2.2 Characterization of DSF fibres

2.2.2.1 Morphological properties

The success of degumming process could be analysed by looking at the changes in morphological features of raw silk fibres as well as degummed fibres. In this study, the samples were mounted onto electro-conductive double adhesive carbon tape pasted on a sample holder. The samples were gold coated for 3 min at a voltage of 20 KV in a sputter coating machine (Hitachi E 101, Japan). They were then loaded into SEM machine (FEI Quanta 200 Environmental Scanning Electron Microscope) and images at 5000 X magnification were captured with an accelerating voltage of 15 kV under vacuum. Subsequently, diameters of raw and degummed silk fibres were determined using Image J software. At least 25 random measurements were averaged to derive fibre diameter.

2.2.2.2 Chemical properties

Comparative analysis of chemical composition of raw as well as degummed fibres by EDAX spectroscopy was reported to yield important clues regarding the success of degumming process. For this purpose, both raw and degummed silk fibres were placed on a sample holder with double side adhesive electro-conductive carbon tape. The samples were gold coated for 3 min at a voltage of 20 KV in a sputter coating machine (Hitachi E 101, Japan). They were then loaded into SEM machine equipped with EDAX accessory (EDAX, AMETEK, US) and spectra were recorded highlighting C (Carbon), N (Nitrogen), O (Oxygen), Ca (Calcium) and Si (Silica) elements.

2.3 Preparation and characterization of aqueous reconstituted silk fibroin (RSF)

2.3.1 Preparation of RSF

The degummed silk fibroin fibres were subsequently reconstituted into aqueous soluble form as per Rockwood et al. 2011(Figure 9). For this purpose, 2 g of DSF fibres were filled into a clean glass reagent vial and 8 ml of freshly prepared 9.3 M lithium bromide solution was poured over the stuffed fibres. The vial was incubated in a hot air oven set at 60°C for 4 h with intermittent manual shaking to ensure proper dissolution. The set temperature and

time was strictly followed to avoid batch to batch variation. Subsequently, the resulting solution were carefully poured into a pre-wetted dialysis bag. The dialysis was performed in distilled water at room temperature for 48 h with at least 6 intermittent water changes. The dialysis vessel was kept on a magnetic stirrer (DIAB MS-PB Medilab Tech, Romania) with mild stirring to ensure efficient dialysis. The resultant solution was subjected to centrifugation (Hermle, Type Z326 K, Germany) at 5000 rpm for 15 min to remove any insoluble matter. The resultant clear RSF solution was transferred into a fresh vial and stored at 4 °C for until further use. Some batches of RSF solution was frozen at -85°C (ESCO Lexicon ULT freezer) and lyophilised (Christ Alpha 1-4 LD, Germany) at -50°C for 24 hrs yield RSF sponge.

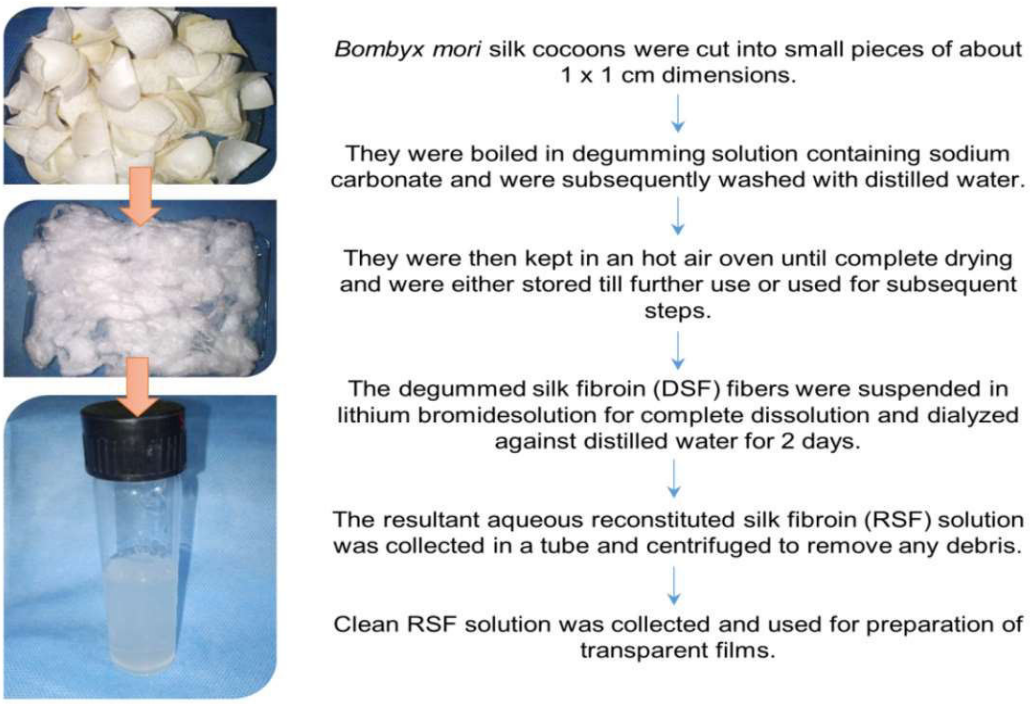

Figure 9. Schematic flow chart for silk processing: firstly, raw silk cocoons were subjected to degumming process to yield fibroin fibres, these fibres were then processed into aqueous soluble silk fibroin solution.

For preparation of films in the following steps, it was critical to determine the concentration of RSF solution. For this purpose, 250 µl of RSF solution was added to a pre-weighed Petri dish and dried in a hot-air oven set at 60 °C for overnight. Once the solution completely dried, the weight of Petri plate was measured again and the RSF concentration was determined by following *Equation* (2), where *Wi* was initial weight and *Wf* was final weight. Subsequently, the solution was diluted to 5% (w/v) with distilled water and stored at 4 °C till further use.

$$Conc.\,of RSF\ (\%, w/v) = (Wf - Wi) \times 4 \times 100 \qquad \textit{Equation}\ (2)$$

2.3.2 Characterization of RSF

2.3.2.1 Molecular weight analysis

Transformation of water insoluble silk fibroin fibre into aqueous reconstituted silk fibroin is typically confirmed by looking at the molecular weight profile of resultant protein solution following SDS-PAGE methodology. In the current study, we performed SDS-PAGE of silk fibroin as per earlier protocol (iGEM Stockholm 2016 SDS-PAGE Lab protocol)) using a vertical electrophoresis unit (Mini-Protean® System, Bio-rad). We used a molecular marker ranging from 11 KDa to 245 KDa supplied by Hi-Media (MBT092-100LN). Detailed protocol with recipes of individual reagents/ buffers used for this study are described in Annexure-I. Briefly, the gel casting unit was assembled with appropriate spacers on an even surface. A 10% separating gel solution and a 5% stacking gel was prepared and used in this study. About 20 µl of RSF sample was mixed up with 5 µl of loading dye and the same was added into the wells. The electrophoresis was run at 80 V until the tracking dye front reached 1 cm above the bottom of the gel. The gel was then stained with Coomassie blue staining solution for about 4 h followed by destaining for overnight. Once clear blue bands were visible, the gel image was captured using a trans-illuminator with white light.

2.3.2.2 Chemical/ structural analysis

The aqueous RSF from water-insoluble silk fibroin fibre also involves molecular transformations in the protein structure that are typically analysed by Attenuated Total Reflectance Fourier-transform infrared (ATR-FTIR) spectroscopy. In the current study, we have performed ATR-FTIR on lyophilized form of RSF and compared the results with DSF fibre. Apart from structural features, FTIR also gives important clues about potential changes in the chemical composition of RSF if any due to aqueous reconstitution process. For this purpose, the RSF and DSF samples were placed on the sample trough and scanned in the range of 4000-400 cm^{-1}wavenumberin ATR-FTIR spectroscope (Nicolet 5700, Nicolet Inc., Madison, USA). Spectra were taken at a resolution of 1 $cm^{-1}$and about 32 scans per sample were evaluated. While the full spectrum was analysed for potential changes in chemical composition in silk fibroin before and after aqueous reconstitution, the spectrum between 1700 – 1600 cm^{-1} was analysed to get insights into structural features.

2.4 Fabrication and processing of RSF films

2.4.1 Fabrication of RSF films

The RSF films were prepared by following a simple solvent casting approach (Figure 10).In the current study, based on the literature, RSF films were prepared by following three different solvents viz. aqueous, HFIP and formic acid that are abbreviated as AQ, HF and FA from here onwards.

For preparing AQ films, after aqueous reconstitution, the concentration of RSF solution was determined and adjusted to 5% (w/v) as detailed in section 2.3.1. Then, 2.5 ml of RSF solution was poured into a clean 35 mm tissue culture dish and the dishes were kept in 37 °C mini incubator (Labnet, US) for overnight drying. After ensuring complete drying, films were carefully collected, air dried and stored in an airtight zip lock covers till further use.

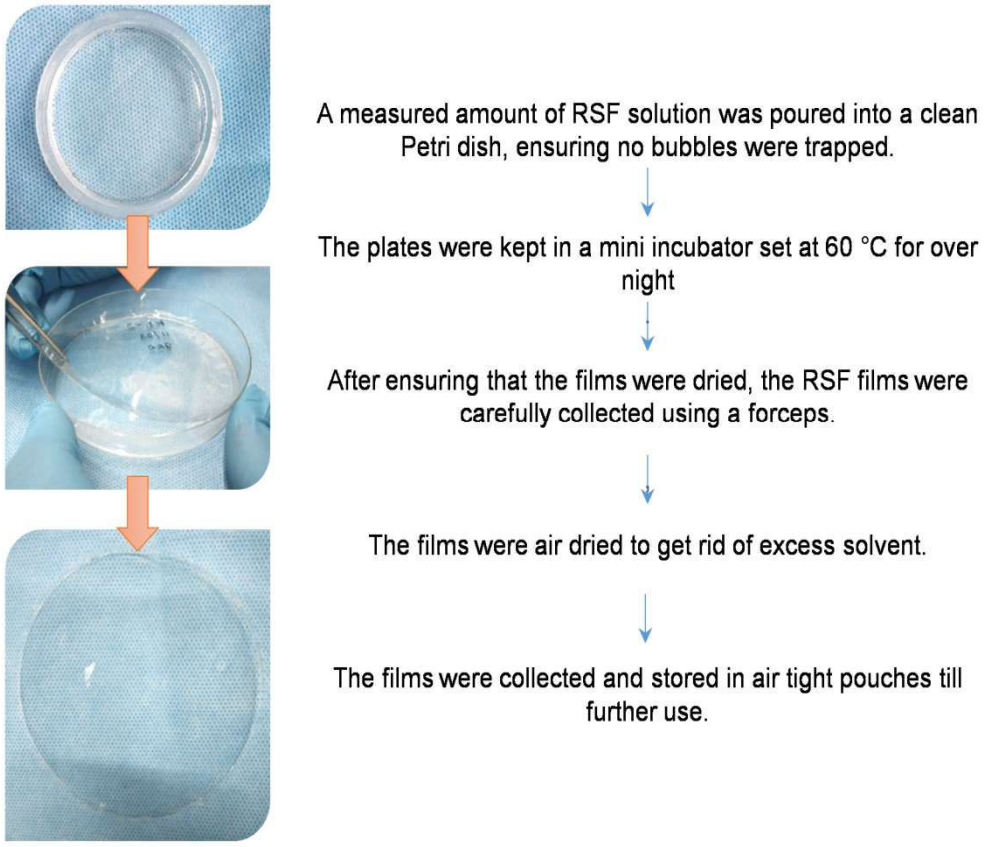

Figure 10. Schematic flow chart of RSF film preparation: RSF solution in aqueous form was poured into petri plates and left for solvent evaporation to yield transparent films.

For preparing HF and FA films, RSF sponge, obtained after lyophilisation process as detailed in section 2.3.1., was dissolved in HFIP and FA respectively to prepare a solution of 5% (w/v). In order to fasten dissolution, the solutions were kept for stirring at room temperature for overnight. After complete dissolution, 2.5 ml of HF and FA based RSF solutions were poured into clean 35 mm tissue culture dishes and kept in 37 °C mini incubator. After overnight drying, HF and FA films were carefully collected, air dried and stored in an air tight zip locks covers till further use.

2.4.2 Post-fabrication processing of RSF films

The solvent cast RSF films prepared by using AQ, HF and FA solvents were further subjected to post-fabrication annealing process to get further insights into process – property relationship in RSF films. For this purpose, based on the literature, we have used three annealing environments viz. water vapour (WA), methanol vapour (MA) and steam (SA).For water vapour and methanol vapour based annealing process, an annealing chamber was setup which includes a big wide mouth beaker with a solid Teflon block placed in the centre and filled with water or methanol sufficient to half immerse Teflon block (figure 11). Subsequently, the RSF films were placed in a Petri dish and the dish was kept on top of Teflon block. The chamber was tightly covered with aluminium foil and plastic cover to restrict vapours from escaping and kept in a mini incubator set at 37°C for 24 h. Subsequently, films were air-dried and stored in zip lock covers till further use.

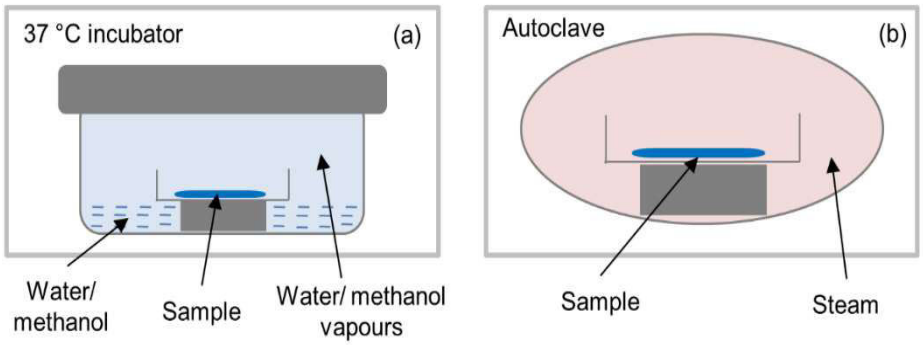

Figure 11. Schematic of post-fabrication annealing process setups: Annealing process was done inside a glass chamber using methanol and water (a) and by autoclaving (b) for enhancing beta sheet structure of protein.

2.5 Characterization of RSF films

2.5.1 Morphological properties

2.5.1.1 Qualitative features

In order to find the effects of fabrication with three different solvents and post-fabrication annealing process in three different environments on morphological features of RSF films, we have performed SEM analysis. Briefly, the films were cut into small pieces (about 0.5 cm^2) and mounted onto an electro-conductive double adhesive carbon tape pasted on a sample holder. Then they were undergone gold sputtering for 3 minutes at a voltage of 20 KV in a sputter coating machine (Hitachi E 101, Japan). They were then loaded into SEM machine (FEI Quanta 200 SEM, US) and images at 5000 X magnification were captured with an accelerating voltage of 15 kV under vacuum. At least three samples were analysed, and a representative picture was presented.

2.5.1.2 Quantitative features

Typically, SEM gives micro-morphological features in qualitative manner, however, in order to find out the effects of process parameters on morphological properties in quantitative terms, we have performed surface profilometry of the films. Briefly, the films were cut into small pieces (about 4 cm^2), placed on sample trough and surface profiles were analysed using a surface profilometer (Taylor Hobson Precision Talysurf CLI 1000). At least three samples were analysed, and the root mean square roughness values (Rq) were presented as averaged values.

2.5.2 Physical properties

2.5.2.1 Surface wettability

Surface wettability is one of the important criteria for any biomaterial candidate. Typically, this is analysed by contact angle measurement. In the current study, the surface wettability of RSF films, fabricated and processed under different conditions, was evaluated by contact angle measurements following a sessile drop technique in a computer-controlled goniometer (OCA 20, Data Physics). Briefly, the films were cut into small pieces (about 1 cm^2) and fixed on glass slide using double adhesive tape. A droplet of 10 µl distilled water was dropped onto the surface of the sample, image was captured within 5 sec and the contact angle was measured using the software supplied with the machine.

2.5.2.2 Water uptake and swelling ratio

Apart from surface wettability properties, it is also important to assess how much water the RSF films can hold, thereby how much they swell, and what are the effects of process parameters on such properties. Water uptake capacity and swelling ratio are typical indices to be analysed. For this purpose, RSF films of 2 × 1 cm size were cut, and the weight of each sample was noted. Each film was immersed in 5 ml ultra-pure water and incubated in a mini incubator set at 37 °C for 24 h. Subsequently, the films were collected, gently wiped with a tissue paper, without exerting pressure, to remove the excess water and the wet weight of the films was recorded. Water uptake capacity and swelling ratio were calculated following *Equation*s (3) and (4) respectively, wherein, W_s denotes swollen weight of the sample and W_d denotes dry weight of the sample.

$$\text{Water uptake (\%)} = \frac{Ws - Wd}{Wd} \times 100 \qquad \textit{Equation} (3)$$

$$\text{Swelling ratio} = \frac{Ws}{Wd} \qquad \textit{Equation} (4)$$

2.5.2.3 Water vapour transmission

Water vapour transmission (WVT) is a critical parameter for biomaterials intended for corneal tissue engineering applications. In the current study, effect of process parameters on WVT of RSF films was analysed as per earlier protocol with slight modification (Zhang et al 2019). Briefly, vials typically used for chromatography were taken and filled with 1 ml of distilled water. RSF films were cut out with a puncher to fit into vented cap of these vials. The initial weight of the assembled vials was recorded, then they were kept in a mini-incubator set at 37°C for 24 h. Vials fitted with a plastic film (OHP sheet) was taken as a control for no permeability and vials with open cap was considered as a control with complete permeability for comparison purposes. The area of the cap vent available for transmission in all cases was 0.28 cm^2. After 24 h, the weight of the vials was noted and WVT calculated as per *Equation* (5) and (6).

$$WVT = \frac{Initial\ weight - final\ weight}{(Area \times Time)} \qquad \textit{Equation} (5)$$

*WVT% = (WVT of test film / WVT of open system) * 100* *Equation (6)*

2.5.3 Chemical/ structural properties

To assess the effects of process parameters on chemical composition as well as structural features of RSF films we have performed ATR-FTIR spectroscopy. For this purpose, the

RSF films prepared with different processing conditions were placed on the sample trough and scanned in the range of 4000 - 400 cm^{-1} wave number in an ATR-FTIR spectroscope (Nicolet 5700, Nicolet Inc., Madison, USA). Spectra were taken at a resolution of 1 cm^{-1} and 32 scans per sample were evaluated. While the full spectrum was analysed for potential changes in chemical composition due to processing, the spectrum from 1700 to 1600 cm^{-1} was analysed to get insights into structural features.

2.5.4 Optical properties

Optical clarity and transparency is the top most qualifying criteria for any artificial or bio-artificial corneal substitutes. Determining the optical properties of RSF films, particularly analysis of process parameters influence on optical properties was our top priority since the RSF films prepared in the current study were intended for applications in corneal tissue engineering. The optical properties of RSF films prepared by different processing conditions were determined by following three approaches: firstly, by visual inspection, secondly by analysing the absorbance spectra ranging UV and visible spectrum, and thirdly by determining transmission (%) across UV-A, UV-B, UV-C and Visible ranges. In all three approaches, the readings were recorded both in dry state as well as in wet state of the film in order to mimic native wet-state physiological condition of cornea. Additionally, a 4-week long study was performed in simulated tear fluid (STF) to track changes in optical properties of RSF films.

2.5.4.1 Visual observations

RSF films prepared by different processing conditions were cut out with a puncher and placed on top of a paper printed with an alphabet. The gross scale photograph was taken using a digital camera. The same samples were incubated in distilled water at room temperature, and after 5 h, the samples were blotted in a clean tissue paper. They were then placed on top of same printed paper and photograph was captured using a digital camera.

2.5.4.2 Absorbance spectra

RSF films prepared by different processing conditions were cut out with a puncher into 4 mm size. They were placed carefully into wells of 96 well tissue culture plate. Absorbance spectrum was read for each sample in UV-Visible range from 200 to 700 nm in a multi-well plate reader (Biotech reader, USA). Subsequently, samples were wetted with 100 µL of distilled water and incubated at room temperature. After 5 h, distilled water was

removed from the wells using micro pipette without leaving any droplet. The spectra were read again in wet state in a multi-well plate reader for same spectral range.

2.5.4.3 Transmission (%)

RSF films prepared by different processing conditions were cut out and placed in a 96 well plate as above. Absorbance of each sample in dry state was recorded at 250, 300, 350 and 500 nm that are representative of UV-C, UV-B, UV-A and Visible spectra in a multi-well plate reader. The samples were processed similar to above study and the absorbance in wet state was recorded for the same wavelengths. Subsequently, the transmission (%) was determined by following *Equation* (7).

$$Transmission\,\% = 10\hat{}(2 - absorbance) \qquad \textit{Equation (7)}$$

2.5.4.4 Transmission (%) – long term study in STF

RSF films, prepared by different processing conditions from the above study were taken and placed in a 96 well plate and continued this study. Here, 100 µL of freshly prepared STF (NaCl- 0.68 g, $NaHCO_3$- 0.22 g, KCl- 0.14 g, $CaCl_2.2H_2O$- 0.008 g, deionised water- 100 ml) was added to each sample and they were incubated in a mini-incubator set at 37 °C. At weeks 1, 2, 3 and 4, absorbance of each sample was recorded at 250, 300, 350 and 500 nm, that are representative of UV-C, UV-B, UV-A and visible spectra, in a multi-well plate reader. Transmission (%) was calculated following *Equation* (7) and the data was compared as a function of time.

2.5.5 Biological properties of RSF films

2.5.5.1 Degradation properties

RSF films were made of silk fibroin protein and therefore we anticipate proteolytic degradation of RSF films upon implantation *in vivo*. In the current study, to understand the effects of process parameters on the degradation profile of RSF films, we have performed a degradation study involving a protease solution (Wong narat et al 2018). Films incubated in STF and PBS were considered for comparison purposes. Briefly, RSF films (about 1 × 2 cm long) were immersed in 1 ml of protease XIV (1U/ml in PBS, with 0.2% w/v sodium azide), STF (with 0.2% w/v sodium azide), or PBS (1X, with 0.2% w/v sodium azide)and the vials were incubated in a mini-incubator set at 37 °C for 24 h. The films were collected, gently pressed within a clean tissue paper to remove the excess medium and the wet weight of the films was recorded. This weight was considered as the initial weight of the RSF

films. The films were suspended in fresh degradation medium and the samples were incubated in mini incubator. The films were collected and weighed at week 1, 2, 3 and 4; each time fresh medium was replaced. Weight loss was calculated using *Equation* (8).

$$Weightloss\ (\%) = \frac{Initial\ weight - final\ weight}{Initial\ weigh} \times 100 \qquad \textit{Equation}\ (8)$$

2.6 Corneal cell culture studies using RSF films

2.6.1 Cytotoxicity study

Before proceeding with corneal cell culture, the RSF films prepared by different processing conditions were subjected to cytotoxicity study as per ISO 10993-5 test on extract assay using a L929 cell line (Mouse subcutaneous connective fibroblasts, obtained from American Type Culture Collection, USA). For this purpose, RSF films were cut into 3 × 1 cm sized dimension so as to get a surface area of 6 cm^2 and they were sterilized by ethylene oxide (ETO) approach. Each film was rinsed with 1× PBS for 3 times, then suspended in 1 ml of DMEM with serum, and incubated in an orbital shaker incubator set at 37 °C and 100 rpm for 24 h. Meanwhile, sub-confluent L929 cells cultured in T25 tissue culture flasks were trypsinized, about 1 × 10^4 cells were seeded per well in 96 well culture plate and incubated in CO_2 incubator set at 37 °C with >90% relative humidity and 5% CO_2 for 24 h. Subsequently, 100 µL of RSF film extracts in culture medium (100 % extracts) were added to test wells. Phenol diluted to 0.13% w/v was prepared freshly in serum-free DMEM and was added to control wells. This was considered as a positive cytotoxic control. Cells fed with complete medium were considered as non-cytotoxic control. Then the plate was incubated for another 24 h in CO_2 incubator. The medium was then replaced with 50 µl MTT reagent (1 mg/ml in serum-free DMEM) and incubated for 4 h in a CO_2 incubator. Resultant formazan crystals were dissolved in 100 µl Isopropanol and absorbance was taken at 570 nm in a plate reader (Biotech reader, USA) (medium mixed with MTT solution was considered as blank). Metabolic activity (%) was calculated using *Equation* (9).

$$Cellviability\ (\%) = \frac{Absorbance\ of samples}{Absorbance\ of cell\ control} \times 100 \qquad \textit{Equation}\ (9)$$

2.6.2 Corneal cell culture studies

Finally, in order to evaluate the feasibility of RSF films for potential applications in corneal tissue engineering, we have performed cell culture studies with SIRC (*Statens Serum institut Rabbit Cornea*) cells obtained from National Centre for Cell Science, Pune,

India. For this purpose, RSF films prepared from AQ, HF and FA approaches were punched into 8 mm circular discs, clipped into cell culture inserts suitable for 24 well plate (Cell Crown^{TM}, Corning) and sterilized by ETO method. Before use, each film clipped onto the insert was rinsed with PBS for 2 times then with medium for 1 time. They were then pre-saturated with fresh DMEM with serum and antibiotics for overnight in a CO_2 incubator. Subsequently, the medium was removed from the wells and 200 µl of SIRC cell suspension containing about 10,000 cells were seeded onto the top chamber of the inserts. Then, 500 µl of cell-free DMEM was added to the bottom chamber of the inserts. Same number of cells seeded on 24 well cell culture plate was considered as a control. The cells were incubated in a CO_2incubator for 24 h. The cell viability was determined by Alamar blue assay as per manufacturer's protocol. Briefly, 500 µl of Alamar blue reagent was added to each well and incubated in a CO_2 incubator for 4 h. About 150 µl was taken into a fresh 96-well plate and the absorbance was read at 570 nm with path length correction at 600 nm in a plate reader.

The cell viability% was determined as per *Equation* (10), where, O1 was molar extinction coefficient (E) of oxidized alamar blue at 570 nm = 80586, O2 was E of oxidized Alamar blue at 600 nm = 117216, A1 was absorbance of test wells at 570 nm, A2 was absorbance of test wells at 600 nm, P1 was absorbance of positive growth control well (cell control) at 570 nm, P2 was absorbance of cell control at 600 nm.

$$\%\ \text{Reduction of alamar Blue Reagent} = \frac{(\mathbf{O2\ x\ A1}) - (\mathbf{O1\ x\ A2})}{(\mathbf{O2\ x\ P1}) - (\mathbf{O1\ xP2})} \times 100 \qquad \textit{Equation}\ (10)$$

Further, to get insights into the qualitative aspects of cell response towards RSF films, we have performed a cell adhesion study followed by staining for cytoskeleton and nucleus. For this purpose, RSF films were clipped to the inserts, ETO sterilized and pre-saturated as detailed in previous section (2.6.2.). Then, SIRC cells (1×10^4 cells) were seeded and cultured on the test material for 24 h in a CO_2 incubator. Cells cultured on standard multi-well plate were considered as control. Subsequently, the cell-laden test material as well as control dish were subjected to staining and imaging. Briefly, samples were washed with 1× PBS for 3 times, fixed in 4% paraformaldehyde for 1 h at room temperature, washed with PBS for 3 times, treated with 0.1 % triton X 100 for 3 min and washed with PBS for 3 times. Cells were stained with Rhodamine - phalloidin (1:100) for 15 min, washed with PBS, counter stained with Hoechst (0.005% w/v in PBS) for 1 min, washed with PBS and imaged in fluorescence microscope (Leica DMI 6000B).

Subsequently, the cell adhesion was also examined by SEM analysis. For this purpose, cell laden films were fixed using 4 % paraformaldehyde for 1 hr. Then, the samples were washed with PBS for 5 minutes (dissolving 1.4 ml 0.2 M NaH_2PO_4 and 3.6 ml 0.2 M Na_2 HPO_4 and 5 ml Millipore water). Further, the samples were dehydrated twice using 30%, 50 %, 70%, 90% and 100% alcohol respectively for 5 minutes each. The samples were then treated with isoamyl acetate, followed by critical point drying and gold coating prior to SEM analysis.

2.7 Statistics

Typically, at least four replicates for each value were averaged and represented as mean ± SD. Statistical differences were analysed by students paired t-test. Differences were considered significant at p value < 0.05 and denoted using * mark. Qualitative images were representative of the respective group.

Chapter 3: Results and Discussion

3.1 Results

3.1.1 Characterization of degummed silk fibroin

B. mori silk cocoons were collected from a local farmer based in Palakkad, Kerala, India and were subjected to degumming process as per a previously reported protocol (Rockwood et al). About 5 g of raw silk cocoons pieces were initially taken for degumming, and after the degumming process, the weight of the resultant DSF was noted to calculate the yield %. In the current study, the yield percentage was found to be 68.6±0.115 %. Our results match with the reported literature wherein fibroin and sericin contents were about 75% and 25% respectively (Qi et al 2017).

3.1.1.1 Morphological properties

Successful removal of sericin, calcium oxalate crystals and other contaminants in silk cocoons is typically analysed by looking at morphological features of silk fibres. In this study, we have performed SEM analysis of DSF and compared the features with raw silk fibres. A quick and gross scale observation indicates transformation of pale raw cocoons into lustrous fibres after degumming (Figure 12a and 12b). Upon SEM analysis, the micro-morphological features including fibre diameter and other details were observed (Figure 12a', 12a" and 12b', 12b"). The raw silk fibres showed particulate matter which could be Calcium oxalate crystals that are typically found in silk cocoons, whereas, such crystals were absent in degummed fibres. Image J analysis of SEM images revealed that the raw fibres had a diameter of 27 ± 1 μm, whereas, the DSF fibres had a diameter of 13 ± 1 μm, thus indicating a reduction in fibre diameter after degumming.

3.1.1.2 Chemical properties

The morphological features from SEM indicated presence of crystal-like structures which could be calcium oxalate crystals or other contaminants. To confirm this indication, the raw cocoon and DSF fibres were analysed by EDAX spectroscopy. The EDAX spectrum of raw silk fibres (Figure 13a) showed peaks at 0.277 KeV, 0.525 KeV and 0.392 KeV that represent carbon (C), oxygen (O) and nitrogen (N) respectively. The raw fibres also showed a peak at 3.690 KeV representing calcium (Ca), and thus, confirmed the presence of calcium oxalate crystals as observed by SEM. In contrast, the EDAX spectrum of DSF fibres (Figure 13b) showed peaks for C, O and N, but no peak was observed for Ca presence. Therefore, both SEM and EDAX collectively confirm the successful removal of sericin, calcium oxalate crystals and other contaminants.

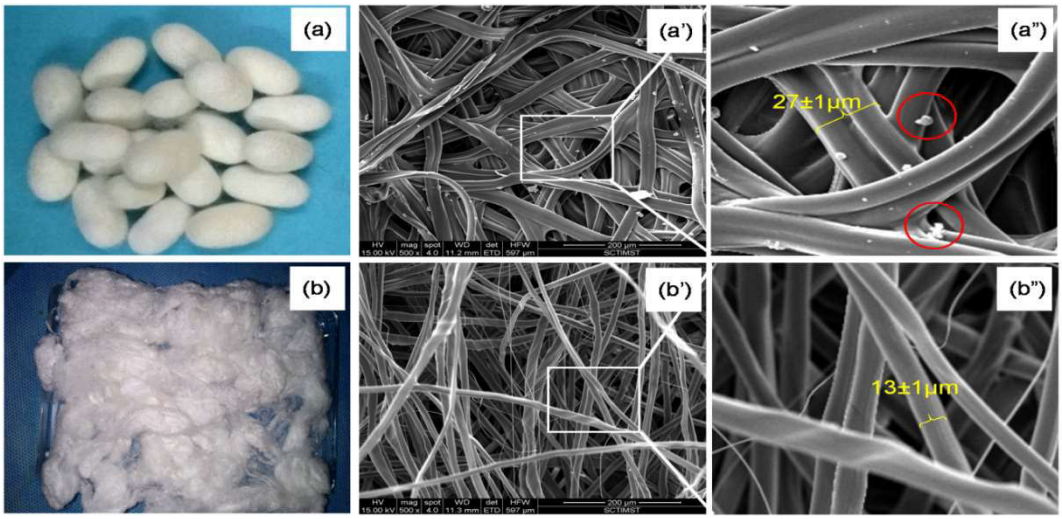

Figure 12. Morphological features of raw and degummed silk fibres: Visual images of(a) cocoon and (b) degummed fibre, and SEM images of (a', a") raw and (b', b") degummed fibre indicated successful degumming (red circles indicate calcium oxalate crystals and fibre diameter highlighted yellow).

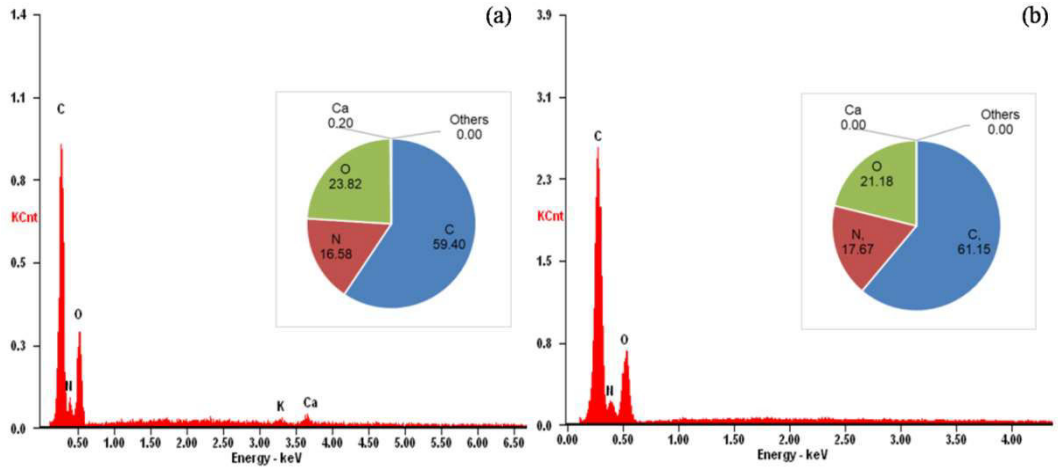

Figure 13. Chemical features of raw and degummed silk fibres: Raw silk fibres (a) from *B. mori* silk cocoons showed C, N, O and Ca peaks, indicating the presence of calcium oxalate deposits, whereas, DSF (b)showed only C, N and O peaks. Inset shows a pie diagram representing the relative atomic percentages of elements in each case.

3.1.2 Characterization of reconstituted silk fibroin

3.1.2.1 Molecular weight analysis

The degummed silk fibres were dissolved in lithium bromide and dialysed against water as per a previously reported protocol (Rockwood et al). The resultant RSF solution was subjected to SDS-PAGE with 10% separating gel and 5% stacking gel followed by staining

with Coomassie brilliant blue as per a previously reported protocol (iGEM Stockholm 2016 SDS-PAGE Lab protocol). The results, as presented in Figure 14, showed a band >245 KDa and thus indicated the presence of heavy chain (H-chain) of silk fibroin. Faint low molecular bands at about 20KDa were also seen in the gel (bands were clear to naked eye compared to images). This could indicate the L-chain (light chain) or P25 unit of RSF.A continuous smear pattern covering a large array of molecular masses was noted. This indicates the polymeric and polydisperse nature of RSF as a result of degumming and dissolution.

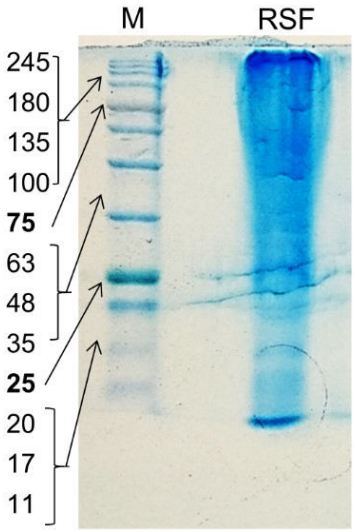

Figure 14. SDS-PAGE pattern of reconstituted silk fibroin: A prominent band >245 KDa and faint bands at about 20 KDa were noted indicated the presence of H, L and P25 subunits of RSF (M – marker ladder).

3.1.2.2 Chemical/ structural analysis

The process of aqueous reconstitution of degummed silk fibres into solution form involves conformational changes in silk fibroin protein structure without adverse effects on overall chemical compositions. To this end, in the current study we have performed ATR-FTIR analysis of RSF (in lyophilized form) and compared the features with DSF fibres. As presented in Figure 15, the DSF fibres showed peaks at 1620 cm^{-1} indicating amide I (C = O stretching), at 1512 cm^{-1} indicating amide II (N-H bending), and at 1226 cm^{-1} indicating amide III (C-N stretching), whereas, RSF showed peaks at 1640 cm^{-1} (amide I), 1517 cm^{-1} (amide II), and 1232 cm^{-1} (amide III). A closer look at the amide I spectra indicated a shift from 1620 to 1640 cm^{-1} after aqueous reconstitution, which indicated conformational transition in silk fibroin from a rigid beta-sheet rich form to less organized

random coil form. Further, there were no noticeable loss or gain in spectral pattern and thus suggested that the overall composition of RSF remain the same as compared to DSF.

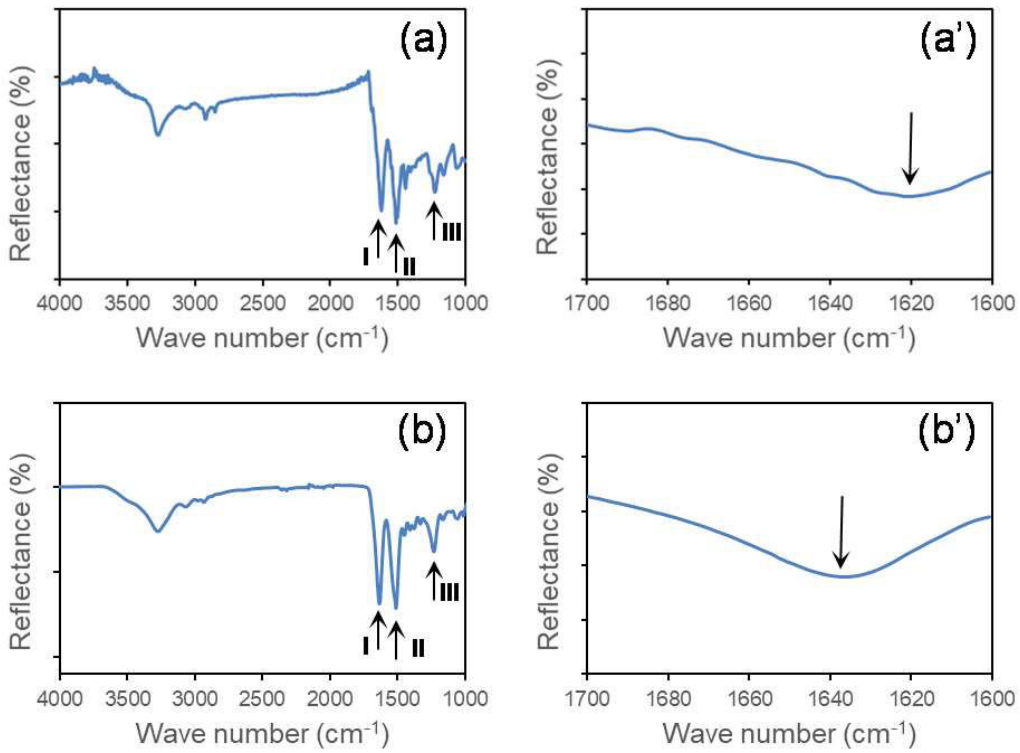

Figure 15. FTIR spectral pattern of silk fibroin before and after reconstitution: Both DSF (a) and RSF (b) showed peaks for amide I, II and II, however, peak position of amide I shifted from 1620 cm^{-1} to 1640 cm^{-1} after aqueous reconstitution.

3.1.3 Morphological properties of RSF films

3.1.3.1 Qualitative features

The RSF solutions prepared using AQ (aqueous), FA (formic acid), HF (HFIP) solvents were casted into films. Subsequently, they were subjected to post-fabrication process involving annealing in methanol (MA), steam (SA) and water (WA). Morphological properties of films were analysed by SEM. As presented in Figure 16, AQ films showed relatively rougher surface with bit of particulate matter, FA showed rough surface with a few pits here and there, and HF films showed smooth surface without any detectable artefacts. However, there were no detectable changes in surface morphology of the films after annealing process in all the samples.

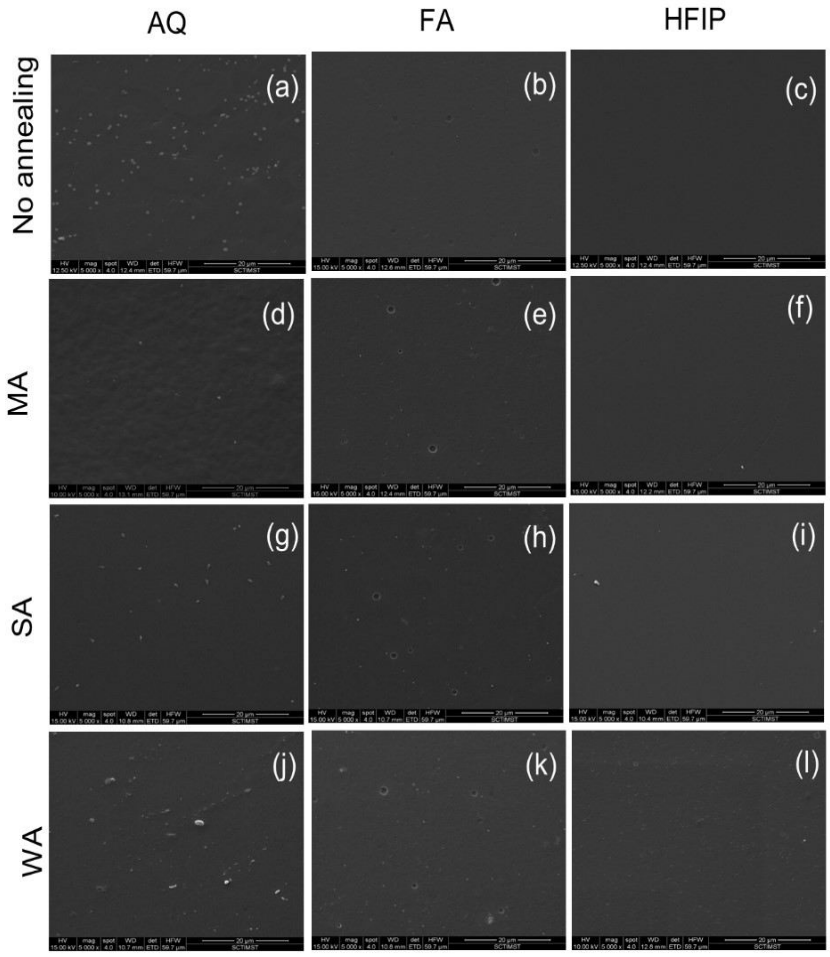

Figure 16. Morphological analysis of silk fibroin films: SEM images of AQ films (a, d, g, j), FA films (b, e, h, k) and HFIP films (c, f, i, l) without and with annealing conditions.

3.1.3.2 Quantitative features

Further insights into topographical features of RSF films were obtained by surface profilometry which provides roughness values in quantitative terms. As presented in Figure 17, root mean square roughness factor (Rq) for AQ, FA and HF were found to be1.39,0.32 and 0.13 respectively. This data confirmed the gross scale roughness profile observed in SEM showing greater roughness in AQ, followed by FA and HF. With respect to the effect of annealing on roughness factor, AQ, FA and HF films showed nearly50% reduction in roughness factor after annealing process in general. For instance, Rq of AQ films reduced from 1.39 to 0.70, Rq of FA films reduced from 0.32 to 0.10 and Rq of FA films reduced from 0.13 to 0.06. Therefore, the topography was affected by, or in other words can be modulated by, fabrication as well as post-fabrication process parameters.

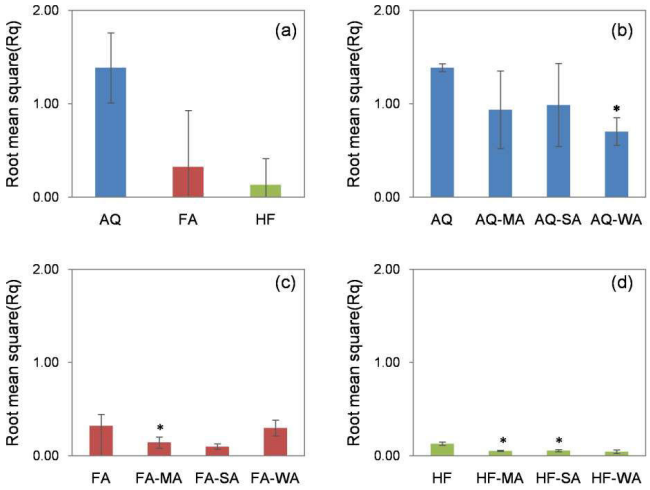

Figure 17. Surface roughness of silk fibroin films: The average surface roughness (Rq) of RSF films without and with post-fabrication annealing process (a – without treatment, b-d with treatment, b – AQ films, c – FA films and d – HF films) (* denotes statistically significant data with p value less than 0.05)

3.1.4 Physical properties of RSF films

3.1.4.1 Surface wettability

Table 1. Effect of process parameters on contact angle (°) of RSF films

Surface wettability is a critical parameter to be determined for any biomaterial intended for use in tissue engineering applications. Typically, this gives an idea about hydrophilicity/ hydrophobicity of the material and thereby defines the cell – material interactions. Typically, this is measured by determining the surface contact angle. In the current study, we have followed using sessile drop technique in a computer-controlled goniometer to determine effect of process parameters in contact angle of SF films. As presented in Table 1, AQ, FA and HF derived films showed contact angle of about 73°, 85° and 89° respectively. All the films were hydrophilic, however, contact angle increased in the order of AQ < FA < HF. Upon post-fabrication annealing, the contact angle was enhanced in AQ films, whereas in FA and HF films it was reduced.

Table 1. Effect of process parameters in contact angle of RSF films

	Con	MA	SA	WA
AQ	72.9±0.8*	76.55±2.7	88.7±2.6*	73.8±1.4
FA	85.05±1.7*	83.4±1.8	75.5±2.4*	74.7±1.5*
HF	88.9±9.3	85.9±2.6	84.4±2.2	93.9±1.6

(* denotes statistically significant data with p value less than 0.05)

3.1.4.2 Water uptake and swelling ratio

Besides surface wettability, it is also important to analyse the bulk wettability i.e. the water uptake capacity of a biomaterial. Besides, it is equally important to evaluate swelling property of the biomaterial. In the current study, we have determined water uptake% and swelling ratio by determining the amount of water absorbed and the weight gained using *Equation*s (3) and (4) respectively. As shown in Table 2, AQ, FA and HF derived films exhibited water uptake% of about 57%, 28% and 27% respectively. Upon post-fabrication annealing, the water uptake% was reduced among all the samples, wherein steam-annealed (SA) samples showed the lowest water uptake% values. Similarly, as presented in Table 3, the swelling ratio was 1.58 in AQ films and it was reduced to 1.28 in FA and 1.22 in HF films. In general, upon annealing the swelling ratio was reduced, wherein steam-annealed (SA) samples showed the lowest swelling ratio.

Table 2. Effect of process parameters in water uptake% of RSF films

	Con	MA	SA	WA
AQ	57.6±4.7	51.8±1.1	23.3±0.3	42.8±3.2
FA	28.3±4.8	29.5±1.7	14.2±1.8	22.6±1.1
HF	27.3±0.1	23±2.9	16±2.9	24.7±0.3

Table 3. Effect of process parameters in swelling ratio of RSF films

	Con	MA	SA	WA
AQ	1.58±0.05	1.52±0.01	1.23	1.43±0.03
FA	1.28±0.05	1.3±0.02	1.14±0.02	1.23±0.01
HF	1.22±0.1	1.28±0.09	1.16±0.03	1.25

3.1.4.3 Water vapour transmission

WVT is calculated to understand the transmission of water vapours through a biomaterial, typically in the form of films. In the current study, we determined WVT% by calculating the loss of water kept in a vial having a lid fitted with RSF films and *Equation* (5 and 6). A vial without any lid was considered as a control. The results are presented in Table 4. AQ

films showed WVT% of 35%, FA showed 25% and HF showed 22% with respect to control. Upon annealing, WVT% reduced in AQ films, but enhanced in FA and HF films.

Table 4. Effect of process parameters in WVT% % of RSF films

	Con	MA	SA	WA
AQ	34.60%*	59.15%*	29.65%	33.61%
FA	25.57%	27.10%	33.28%	30.65%
HF	22.58%	26.16%	24.63%	27.10%

Closed system: 0.30%, Open system: 100%, Dialysis membrane: 66.08%

(* denotes statistically significant data with p value less than 0.05)

3.1.5 Structural/ chemical properties of RSF films

3.1.5.1 Absorbance spectra of films without post processing.

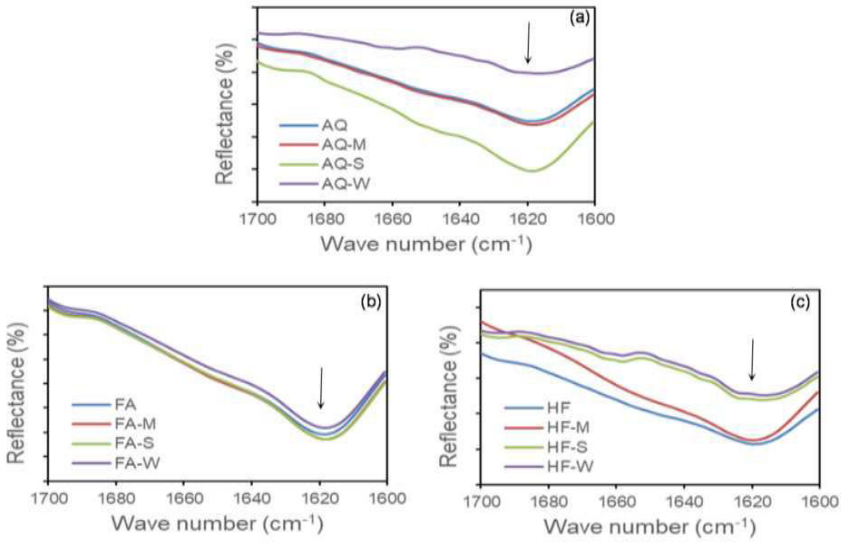

Figure 18. ATR-FTIR spectral data of silk fibroin films: silk fibroin films showing spectra depending upon their processes and post processing parameters, Controls- AQ (a), FA (b), HFIP (c).

Chemical properties of RSF films were also obtained to determine the chemical groups present in them after processing, which was also compared after post processing treatments. AQ (a), FA (b) and HFIP (c) samples. in figure 15 the RSF showed a characteristic peak at 1640 cm^{-1} which shows a shift from highly ordered beta sheet to less ordered random coil structure. After processing and post processing, the films were again analysed for FTIR characterisation and found all films irrespective of processing

parameters showed a peak at 1620 cm^{-1}as in figure 18 which is an indication of conformational change in structure from less ordered random coil to highly ordered beta sheet structure. While analysing chemical characteristics, none of the modifications were observed. After post fabrication annealing, no new peaks or no deletion of characteristic peaks were observed and thus denotes the unaltered chemical/structural properties.

3.1.6 Optical properties of RSF films

3.1.6.1 Visual observations

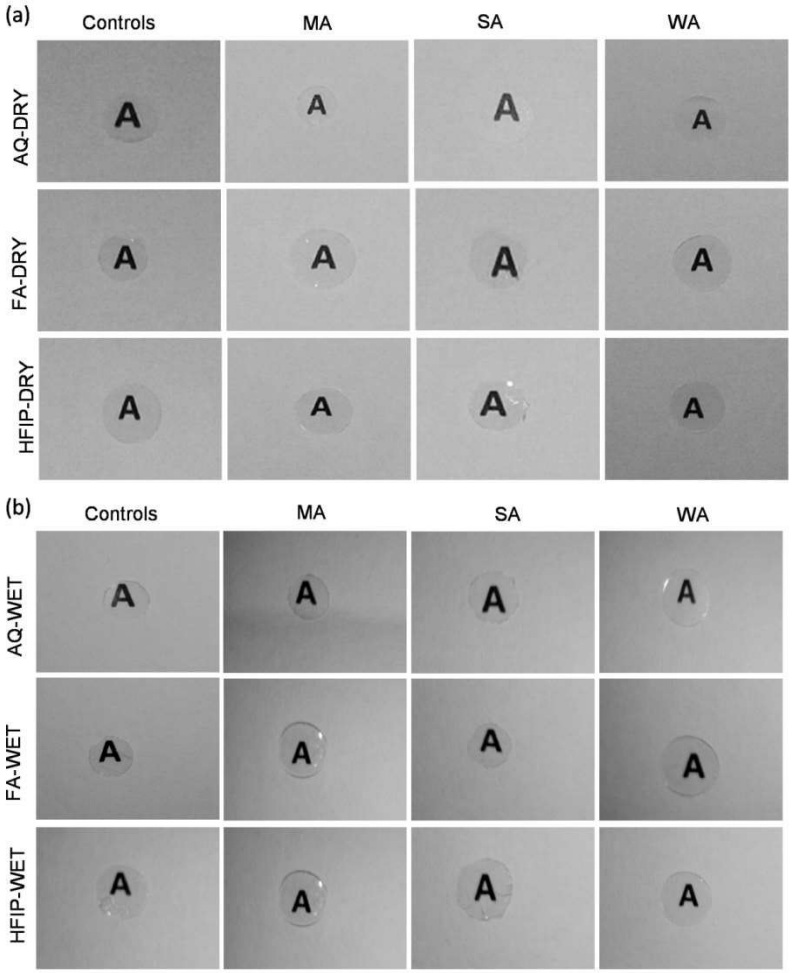

Figure 19. Optical clarity of silk fibroin films: AQ, FA and HF derived SF films (without annealing and annealing with methanol (MA), steam (SA) and water (WA)) showed excellent optical clarity in (a) dry state as well as in (b) wet state.

Optical clarity is the foremost criterion for consideration while designing a biomaterial for corneal tissue engineering applications. Therefore, in this current study, we have focused on the optical properties and investigated if there were any process (fabrication and post-fabrication) dependant variations. As presented in Figure 19, RSF films from all three

solvents such as AQ, FA and HF, with and without annealing, showed excellent optical clarity. Typically, in the native state, cornea was covered with tear film and therefore remains in wet state at all times. To this end, we have incubated RSF films in water and recorded the changes in optical clarity after wetting. As presented in Figure 19, RSF films showed remarkable optical clarity even in wet state, irrespective of processing conditions.

3.1.6.2 Absorption spectra

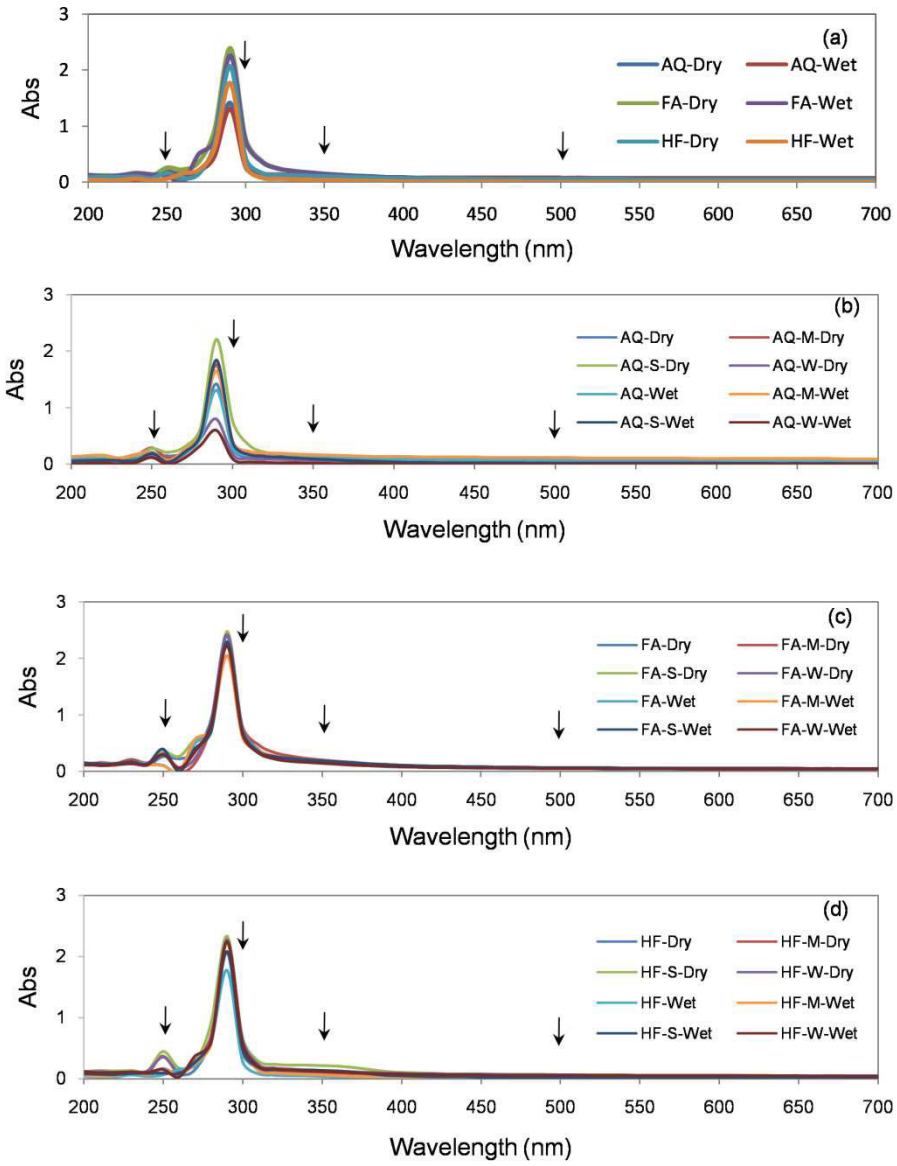

Figure 20. UV – Vis spectral data of silk fibroin films: The absorption spectra of (a) AQ, FA and HF films without annealing, (b) AQ films with and without annealing, (c) FA films with and without annealing and (d) HF films with and without annealing (arrows indicate UVC, UVB, UVA and visible spectra at 250, 300, 350 and 500 nm respectively.

To get further insights into the optical properties, we analysed absorption spectra of RSF films in UV-Visible spectroscopy from 200 to 700 nm wavelength in a multi-well plate reader. As presented in Figure 20, the results indicated that all RSF films in dry state showed almost negligible absorbance in Vis range (500 nm), irrespective of fabrication and annealing process. Subsequently, to simulate the wet state condition of cornea as in natural condition, we have wetted the RSF films and recorded the spectra once again. After wetting, AQ, FA and HF derived films showed no noticeable changes in the overall spectral pattern, across various processing parameters. Similarly, negligible absorbance was recorded at UVA (350 nm) and UVC (250 nm) range whereas relatively high absorbance was recorded at UVB (300 nm) in all the films, both in dry and wet state.

3.1.6.3 Transmission (%)

Further, to get quantitative information on optical properties of RSF films, we have taken spectra at representative wavelengths and calculated transmission%. As presented in Figure 21, similar to previous observation, all RSF films in dry state showed almost 80 – 90% transmission in visible range (500 nm), irrespective of fabrication and annealing process. Subsequently, we have calculated transmission% for wet samples. After wetting, AQ, FA and HF derived films, with and without annealing, showed slight changes in transmission%, across various processing parameters. In the UVC (250 nm) range, RSF films showed about 60 – 80%, however it was decreased with annealing by maximum 2-fold. In the UVB (300 nm) range, RSF films showed about 20 – 40%, however it was decreased with annealing by maximum 3.5-fold. In the UVA (350 nm) range, RSF films showed about 70 – 80%, however it was decreased with annealing by maximum 1.5-fold.

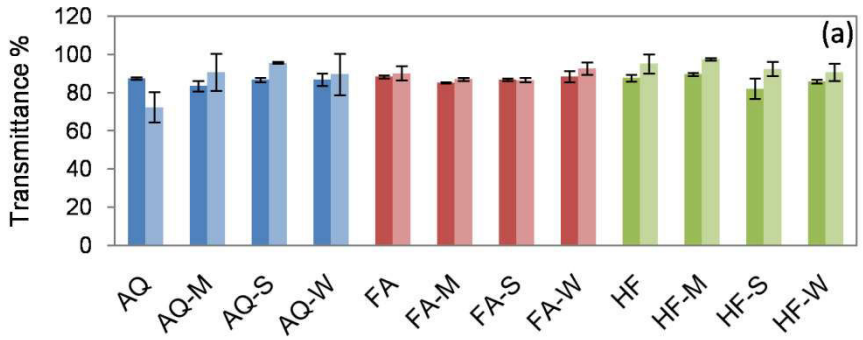

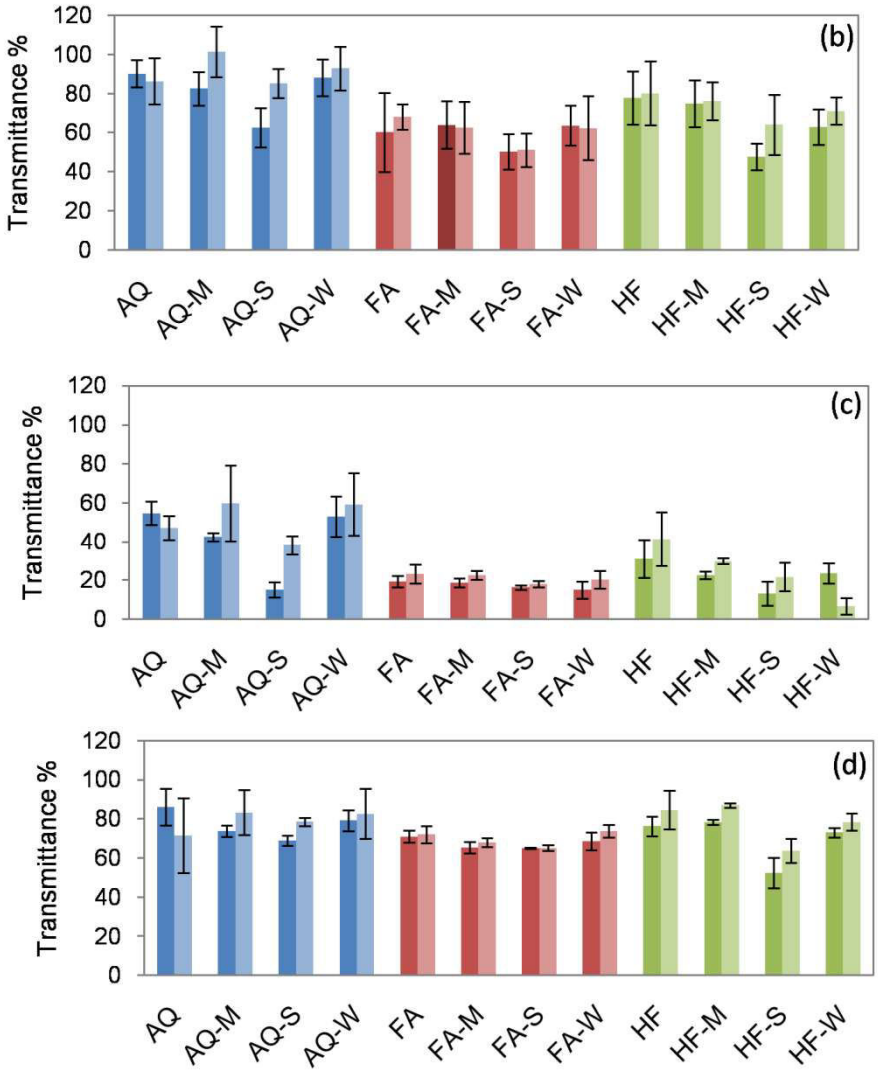

Figure 21. Transmittance% of silk films in dry and wet state: The graph showed difference in absorbance value respective of different wavelengths before and after wetting. The transmission% of AQ, FA and HF films with and without annealing at (a) visible, (b) UVC, (c) UVB and (d) UVA at 500, 250, 300 and 350 nm respectively. Dark bars represent dry state and light bar represent wet state.

3.1.6.4 Transmission (%) – long term study in STF

In order to check if the long term wetting influences the optical clarity of RSF films, we have incubated the films in simulated tear fluid (STF) for 4 weeks, then recorded absorbance at representative UV – visible wavelengths and calculated transmission%. For the sake of simplicity, we have presented Visible range (500 nm) data of week 1 and 4 here (Data for weeks 2 and 3 are not shown. Data for UVA, UVB and UVC is presented as annexure). As presented in Figure 22, all the films (with and without annealing) showed

about 90% transmission and there was no significant difference in transmission% even after 4 weeks of incubation in STF.

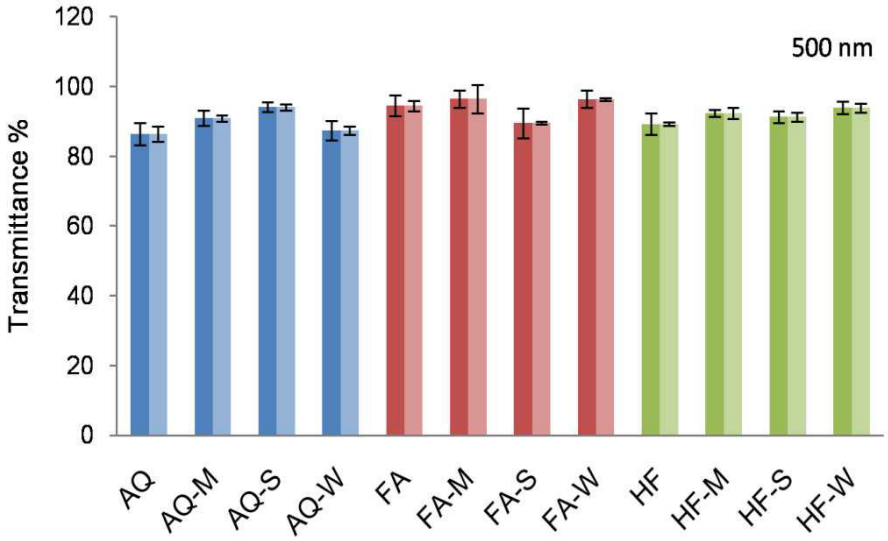

Figure 22. Transmittance% of silk films in STF for 4 weeks: The quantitative data on optical clarity of RSF films at a representative visible range (500 nm) showed no significant changes after incubation with STF for 4 weeks (dark bar shows week-1 data and light bar shows week-4 data).

3.1.7 Biodegradation properties of RSF films

Bioresorbability is a critical parameter for any biomaterial for potential applications in tissue engineering. In the current study, we have analysed degradation profile of a silk fibroin films in three different media over 4 weeks at 37 °C. Here we have used AQ, FA and HF films without annealing only. The weight loss% was determined and presented in Figure 23. Gradual weight loss was noticed in all the films irrespective of the medium. However, at week 4, AQ films showed significantly higher degradation in enzyme solution with a weight loss of about 72%, compared to PBS (12%) and STF (4%). Similarly, HF films showed significantly higher degradation in enzyme solution with a weight loss of about 86%, compared to PBS (5%) and STF (5%). But FA films exhibited only about 12% weight loss in enzyme solution that was close to 7% in PBS and 7.5% STF at week 4.

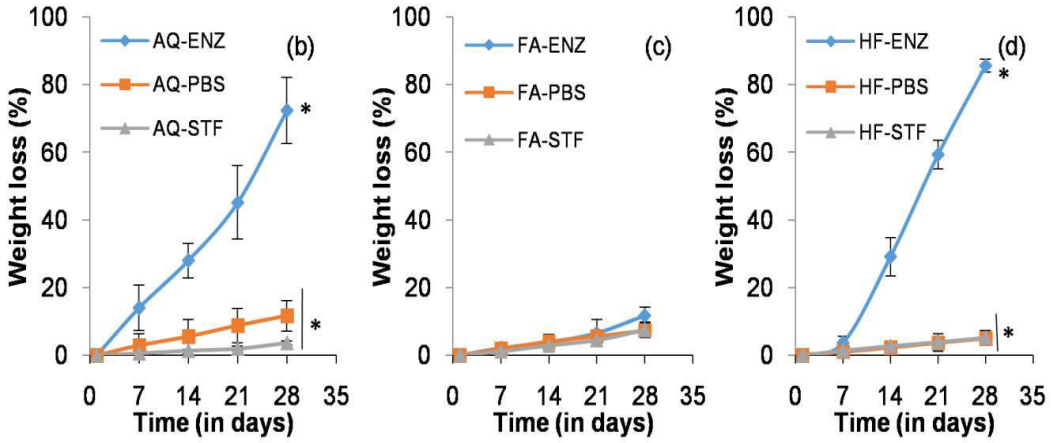

Figure 23. Biodegradation profile of silk fibroin films: Weight loss% values of RSF films in a protease (ENZ), phosphate buffered saline (PBS) and simulated tear fluid (STF) over 4 weeks of incubation. (a – all in one plot, b – AQ plots, c – FA plots, d – HF plots). (* denotes statistically significant data with p value less than 0.05)

3.1.8 Cytotoxicity properties of RSF films

Before proceeding with corneal cell culture studies, we investigated the cytotoxicity of the RSF films prepared by different processing conditions following test on extract and MTT assay as per ISO 10993-5. Test on extract assay is a well-known cytotoxicity assay which involves the microscopic examination of changes in cell morphology in response to test and control samples. As can be seen in the figure, cells treated with the test sample extracts (AQ, FA and HF with and without annealing) showed good morphology similar to that of cell control, therefore they were considered as non-cytotoxic (grade 0), whereas the cells treated with phenol showed severe cytotoxicity (grade 4) with round non-viable cells (only a representative image of test sample is presented). As per ISO 10993-5, grade 2 and more is considered as cytotoxic; since all the test samples showed grade 0 they were considered to be non-cytotoxic.

While MTT assay is used for obtaining quantitative measurement where in mitochondrial dehydrogenase in the live cells reduce water soluble yellow coloured MTT to a water insoluble purple coloured formazan which can be dissolved in isopropyl alcohol and the absorbance can be recorded at 570 nm. Here, higher the absorbance higher the cell viability. In the current study, as presented in figure 24, about 80-100 % cell viability was observed in the test samples, about 100 % cell viability was observed in cell control and < 10 % viability was noted in phenol control. As per ISO 10993-5, the cell viability <60 % is

considered as cytotoxic; since all the test samples showed viability >80 %, they were non-cytotoxic.

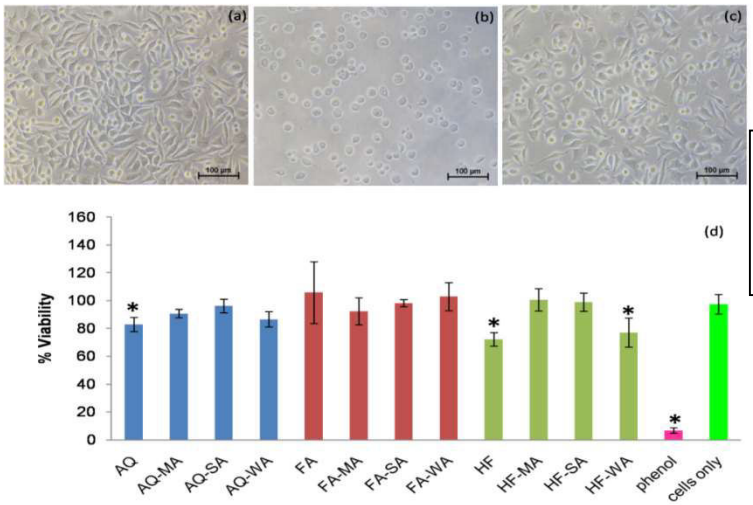

(a) and (c) non cytotoxic (grade 0)
(b) cytotoxic (grade 4)

Figure 24. Cytotoxicity profile of RSF films: Inverted phase contrast image of cells treated with extracts of test sample (a), phenol (b) and cell control (c). Percentage viability of cells as measured by MTT assay(d). (* denotes the statistical significance at p value < 0.05).

3.1.9 Corneal cell culture studies using RSF films

Finally, we have investigated the ability of the RSF films, prepared by different processing conditions, to support corneal cells for subsequent application in corneal tissue engineering. For this purpose, we have cultured SIRC cells (rabbit corneal cells) on RSF films and determined cell viability and cell adhesion with respect to cells cultured on TCPS (tissue culture polystyrene dish). For cell viability, we followed alamar blue assay, which is a quantitative cell viability assay involving metabolic reduction of weakly fluorescent resazurin to highly fluorescent resorufin by viable cells. Here, the absorbance can be recorded at 570 nm using 600 nm as reference wavelength, and higher the absorbance value higher will be the cell viability. In the current study, as presented in figure 25, >70 % cell viability was observed in all the test samples with respect to cells cultured on TCPS. Subsequently, cell laden test samples were stained with cytoskeletal and nuclear stains to check cell adhesion pattern. As presented in figure 26 a good number of cells were found to adhere and well spread on TCPS with typical corneal epithelial morphology. Similarly, the cells on the test samples were found to be well spread with typical corneal epithelial morphology (ovoid to cuboidal) as compared to the control. Subsequently, as shown in figure 27, the SEM analysis of cells laden films revealed that SIRC cells were nicely

adhered and spread on the RSF films similar to that of TCPS. Further, as mentioned earlier sections, optical clarity is the critical characteristic property of a biomaterial for corneal tissue engineering. To confirm the transparency after cell culture studies, the cell laden test materials were visually observed and photographed. As presented in figure 28, all the test samples under study were found to be clear and optically transparent. Overall, the RSF films prepared by different processing conditions, were found to be compatible with corneal cells for potential application in corneal tissue engineering.

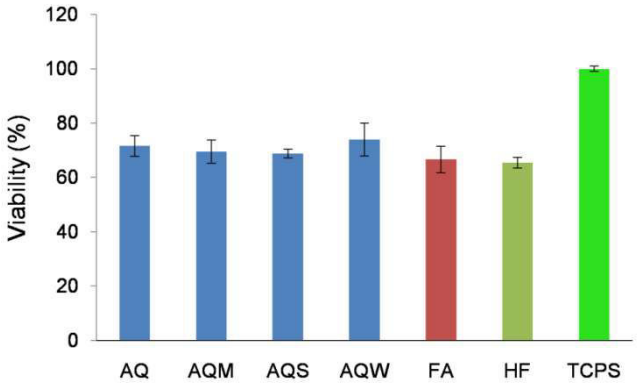

Figure 25. Cell viability % of SIRC cells on RSF films: As compared to the cells on TCPS, >70 % cell viability was observed on the test materials.

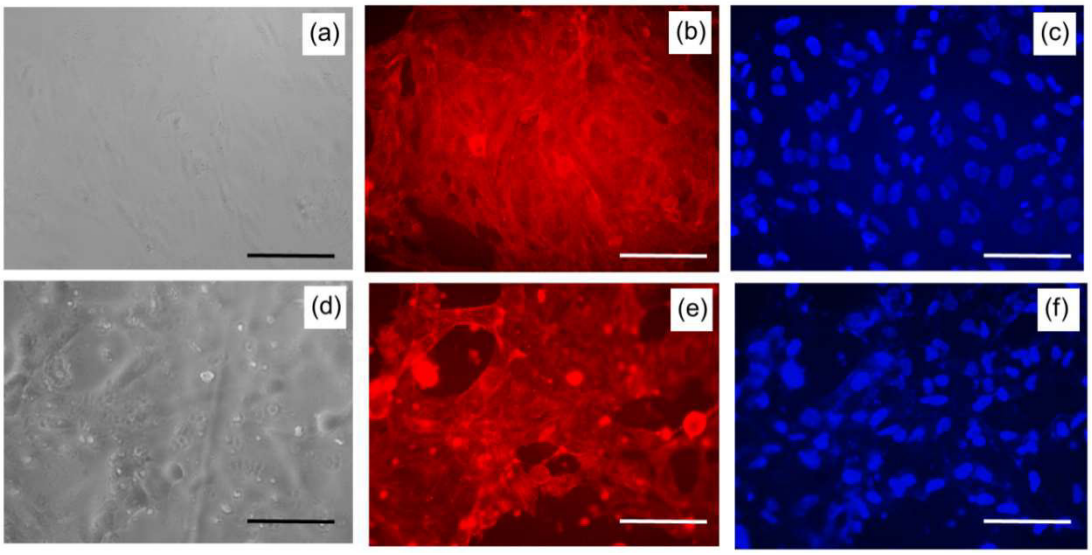

Figure 26. Cell adhesion on SF films: SIRC cells adhered and spread well on SF films similar to that on TCPS control. (a-c TCPS, d-f AQ SF films, a,d phase contrast, b,e cytoskeleton stained with rhodamine phalloidin, c,f nuclei stained with Hoechst).

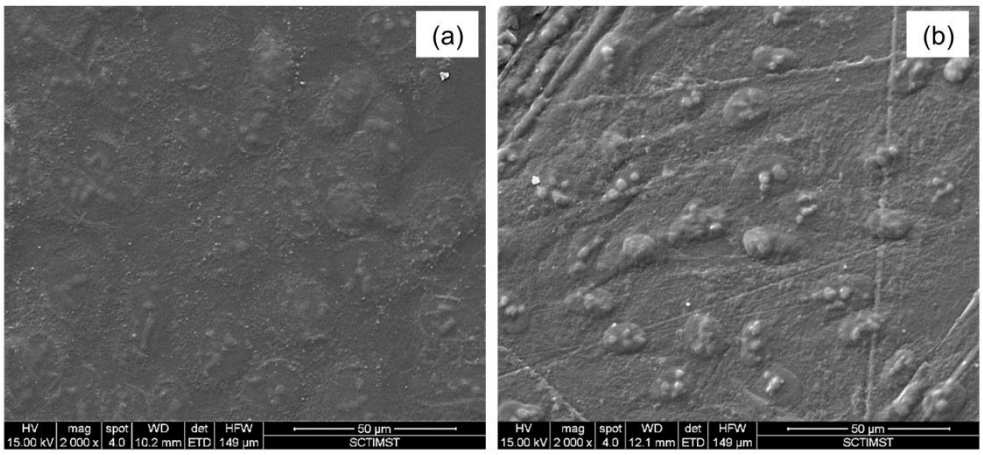

Figure 27. Cell adhesion study: SEM images of SIRC cells on TCPS and AQ silk fibroin films showed well adhered and nicely spread morphology (SEM images of cells on films (a – TCPS, b –AQ RSF films).

Figure 28. Transparency of RSF films after cell adhesion studies: All the test materials were found to retain its original transparency even after cell culture (a - AQ, b – FA, c – HF).

3.2 Discussion

Cornea – a transparent, protective, outermost layer of eye, provides 75% of total refractive power and transmits 98% red light and 90% blue light. It is estimated that over 10 million individuals experience bilateral corneal blindness worldwide owing diseases, age related problems, accidents, etc. Currently, corneal transplantation is the only possible method to restore vision and the success rate of corneal transplantation is 90%, but almost no chance of success in patients with recurrent graft failures. The lack of donors, possibility of infections and rejection rates made researchers to find an alternative method for therapy. To this end, tissue engineering has emerged as an alternative therapeutic approach which involves creation of bio-artificial tissues *in vitro* by culturing cells of patients or healthy donors on a biomaterial scaffold in presence of bioactive growth factors. A tissue engineered cornea replacement could provide significant benefits over donor shortage for corneal transplantation. However, the two major challenges to the field of tissue

engineering in constructing a cornea are: transparency and tissue strength. The array of collage fibres and refractive index of these fibrils by interstitial proteoglycans are responsible for the transparency of cornea. The thickness of stroma and the arrangement of collagen fibres matters for visible light waves to pass through the cornea. The challenges in creating tissue engineered cornea include creating a structure that is biocompatible and bioresorbable (Shah et al., 2008).

The materials which are available in the nature provide an acceptable template to revise, restructure while maintaining its sustainability. Nature always has been serving as a typical example of biological engineer with its simple yet magnificent design that has inspired novel findings, silk is one among those which inspired various scientists and still hits the awe of researchers with its unique properties. Unlike other natural polymers, amenability of silk to be processed into a wide array of formats, suiting for different applications serves an extra credit. Robust mechanical properties, tunable degradation pattern, chemical properties aid its usage in different fields. Due to the presence of additional desirable characteristics, silk fibroin and blends of silk fibroin have gained the attention of scientist all over the world. Although huge number of studies has been performed with silk fibroin in tissue engineering, no study was taken up so far to investigate process dependent variations in silk fibroin films. The current study was aimed to fill the gap and provide insights into fabrication and post-fabrication dependent variations in silk films, particularly in the context of corneal tissue engineering.

With a hypothesis that various fabrication and post-fabrication processing parameters could influence the properties of silk fibroin derived films, we have (i) degummed *Bombyx mori* silk cocoons into silk fibroin fibres and characterized its morphological and chemical/structural properties, (ii) reconstituted the degummed fibres into aqueous silk fibroin solution and characterized its molecular weight and chemical/structural properties, (iii) processed RSF solution in AQ, FA and HFIP into films by solvent casting approach, followed by annealing with methanol, water and steam, and characterized its morphological properties (SEM, surface roughness), physical properties (contact angle, swelling index, water uptake, WVT%),chemical/structural properties (FTIR), optical properties (optical clarity, absorbance spectra and transmission% in UV-Visible range), degradation properties, and finally (iv) evaluated its cytotoxicity with L929 cells and cytocompatibility with SIRC cells to determine its potential application in corneal tissue engineering applications.

The silk fibroin from *Bombyx mori* silk cocoons were secluded by removing sericin, calcium oxalate crystals and other contaminants if any, following Pramod et al. After degumming, we found that the pale raw cocoon fibres turned into lustrous fibres. Morphological analysis by SEM revealed the presence of crystal-like particles in raw fibres, and upon degumming, these crystal-like structures were removed. Previously, Pramod et al has reported presence of crystal-like structures in SEM images of raw cocoon and removal of the same after degumming. Elemental composition analysis by EDAX was done to confirm the composition of crystals observed in SEM. EDAX spectra showed a peak at Kα 3.690 KeV in raw fibres and thus indicated that these crystals were made of calcium oxalate; whereas the degummed silk fibres showed no such peak and thus confirmed successful degumming. Similarly, Kaur et al also found a peak at 3.691 KeV in EDAX analysis in raw cocoons confirming the calcium oxalate crystals and subsequent removal of the same after degumming process. Further, Image J analysis indicated a reduction in fibre diameter from 27 ± 1 µm in raw fibres to 13 ± 1 µm which was due to split up of silk fibre bundle into individual fibers. In a similar study, Mousumi et al also found such reduction in fibre diameter from 15 µm to 6 µm. Our observations were in good agreement with earlier reports.

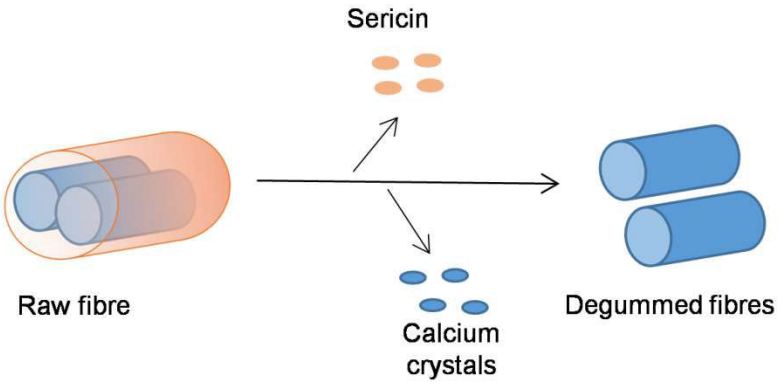

Figure 29. Insights into degumming process: upon treatment with sodium carbonate, sericin, calcium oxalate crystals and other contaminants are removed and thereby the silk fibres become separated.

The DSF fibres were then dissolved in lithium bromide as per earlier protocol by Rockwood et al. Typically, molecular weight of RSF was analyzed by SDS-PAGE and in the current study bands we obtained a band >245 KDa and faint low molecular bands at about 20 KDa. These observations indicated the presence of heavy chain (H-chain) and L-chain (light chain) or P25 unit of silk fibroin. A continuous smear pattern covering a large array of molecular masses was noted. Similar results were obtained by Wang et al 2017

Zafar et al 2015 and Yamada et al. 2001 who reported heavy chain band at >245 KDa and light or P25 chains around 17-30 KDa. Wang et al 2013 also found smear pattern that was attributed to the differential breakdown of silk fibroin polymer chain into variously sized molecules, either during degumming or dissolution. Subsequently, to understand the conformational changes in silk fibroin during dissolution, we performed ATR-FTIR analysis. Both DSF and RSF showed characteristic amide I, II and III peaks, however, amide I spectra indicated a shift from 1620 to 1640 cm^{-1} after aqueous reconstitution. This can be attributed to the conformational transition in silk fibroin from a rigid beta-sheet rich form in DSF to less organized random coil form in RSF. Our results match with Boulet-Audet et al and Sandeep et al 2017who reported similar ATR-FTIR band shift from about 1620 cm^{-1}in DSF to about 1640 cm^{-1}in RSF and attributed the changes to conformational transition in silk fibroin structure.

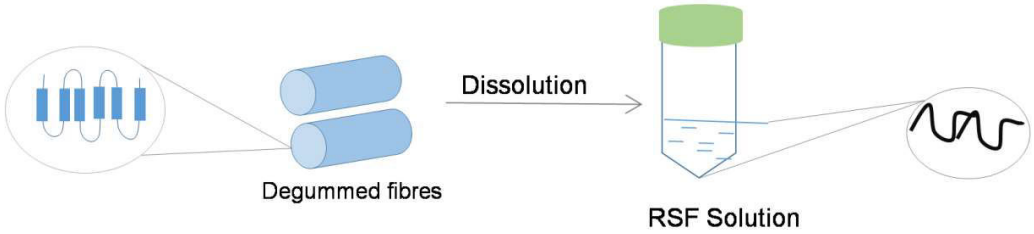

Figure 30. Insights into aqueous reconstitution process: upon dissolution in lithium bromide and subsequent dialysis in water, silk fibroin transforms from silk II (highly ordered structure) to silk I (random structure).

Subsequently RSF was prepared in AQ, FA and HF solutions and the films were obtained by solvent casting approach. They were then subjected to post-fabrication annealing process in methanol, water and steam. Morpho-topological analysis by SEM and surface profilometry revealed a decrease in roughness in the order of AQ (Rq 1.39)> FA (Rq 0.32) > HF (Rq 0.13). This was reduced by nearly 50% after annealing process in general. Recently, Yang et al 2018 reported surface morphology of *B. mori*/ tussah silk fibroin blend films, wherein, they observed smoother surface morphology in FA derived films than AQ derived films. Thus, the process dependent variations in morpho-topological properties of RSF films in our study were comparable with earlier reports. We attribute such changes to the properties of solvent used, including the boiling point as well as SF solubility factor and conformational changes therein.

We then analyzed physical properties of the films such as surface wettability, swelling ratio, water uptake capacity and WVT%. Contact angle measurements indicated that all the films were hydrophilic, however, contact angle increased in the order of AQ (73°) < FA (85°) < HF (89°) and thus indicated a decrease in surface wettability. Water uptake and swelling ratio decreased in the order of AQ (57.6% and 1.58) > FA (28.3% and 1.28) > HF (27.3% and 1.22). WVT% decreased in the order of AQ (35%) >FA (26%) >HF (23%). Zhang et al 2019, Luang budnark et al 2012 evaluated wettability, water uptake, swelling and WVT% and found that the films were hydrophilic, meanwhile, the swelling ratio of the films was in range of 48–57%. They also evaluated silk fibroin films conjugated with curcumin for WVT% and found to have better permeability as that of our results. In the current study, when compared to the films made from AQ, the films made from FA or HF solvents were showing reduced interaction with water in general. Further, upon annealing, compared to FA and HF, the SA annealed films showed reduced interaction with water, as reflected in contact angle, water uptake, swelling ratio and WVT%; this could be due to steam induced conformational changes in SF protein.

Insights into chemical/ structural properties of RSF films were determined by ATR-FTIR spectroscopy. SF in fibre form showed a peak at 1620 cm^{-1} indicating the highly ordered crystalline beta sheet structures (typically mentioned as silk-II form). Upon reconstitution, it showed a shift in peak to 1640 cm^{-1} that corresponds to the presence of less ordered random coil structures (typically mentioned as silk-I form). However, after film preparation, SF showed a reverse shift in peak to 1620 cm^{-1}, irrespective of processing parameters under study, indicating the conformation transition from less-ordered to highly ordered structures. Besides, SF in all the forms showed characteristic peaks for amide I, II and III without any addition or deletion of peaks. This indicates that there were no compositional changes in SF, rather only structural changes were noted. Jaramillo et al. 2017 and Kasoju et al 2016 evaluated the FTIR spectra of SF and reported that SF was characterized by amide I, II and III bands. In particular, amide I band position was explored to get details of secondary structure of SF, where, degummed SF fibre typically showed silk-II structure, which changed to silk-I upon aqueous reconstitution, and then reversed back to silk-II upon processing into films, sponges, etc., which can be relatable to our results.

The visual observation of SF films was done to confirm the optical clarity. All films were found to be optically clear and transparent irrespective of processing

parameters. Absorbance spectra was recorded from 200 to 700 nm in UV-Vis spectroscope and transmission% was determined at UVA (350 nm), UVB (300 nm), UVC (250 nm) and Visible (500 nm) wavelengths. Overall, absorbance spectra (Vis range) of RSF films in dry state showed almost negligible absorbance; After wetting, AQ, FA and HF derived films showed no noticeable changes in the overall spectral pattern, across various processing parameters. However, transmission% in visible range (500 nm) in all RSF films showed almost 90% transmission, irrespective of fabrication and annealing process, and it remained unaltered even after 4 weeks of incubation in STF. Qi et al reported preparation of SF based flexible and conductive films and showed that the films possessed 80 – 90% transmission% even after blending with other components. Yoon et al 2013 reported preparation of SF films with a focus on assessing effects of degumming process parameters on film properties. Here they found excellent transparency in all the films, however, the transparency tends to change after wetting the films. Kaewpiroma and Boonsang 2020 reported influence of alcohol treatment on SF films, wherein they showed that SF films treated with alcohol showed exceptional optical transparency of about 90%. Similarly, Liu et al 2012 and Nor et al also evaluated the transmittance% of SF films and reported about 90% transmission in visible light spectrum. Collectively, these reports fall in line with our observations on SF film optical properties.

Silk films were analyzed for degradation till 28 days in three different media viz. PBS, STF and protease XIV enzyme (ENZ). Weight loss % was higher in AQ films incubated in ENZ (72%) compared to PBS (12%) and STF (4%). Similarly, HF films degraded more in ENZ (86%), compared to PBS (5%) and STF (5%). Whereas FA films exhibited only about 12% weight loss in ENZ, that was close to 7% in PBS and 7.5% STF at week 4. The current study revealed that process parameters influence the degradation time. This could be attributed to the content and balance of silk I and II structures in SF films. Higher the silk II content than silk I, lower will be the degradation and vice versa. In our study, AQ and HF showed higher degradation than FA samples, thus, suggested that silk II component was perhaps less in AQ and HF than FA. Previously, Yao et al. 2004, Ha et al. 2005 and Liu et al. 2018 reported that FA was an attractive solvent for inducing the conformational changes towards β-sheet structure in SF and thereby to modulate the unique properties of SF materials. Although HF was found to induce silk II structure in SF (Zhao et al. 2002), in the current study, it appeared that the silk II component was

relatively less in HF films than in FA films. This has to be looked in details, probably by analyzing the secondary structure details by FTIR spectral deconvolution.

We then studied cytotoxicity of SF films by following test on extract assay as per ISO 10993-5 using L929 cell line. Here, we found that the test samples (AQ, FA and HF with and without annealing) were non-cytotoxic (grade 0), like that of cell control. Subsequent MTT assay showed about 80-100% cell viability in the test samples (AQ, FA and HF with and without annealing), close to that of 100% cell viability in cell control extracts. Our results match with Akturk et al. 2016 who reported about 90% cell viability of L929 cells treated with extracts of silk fibroin/gold nanoparticle 3D matrices as per ISO 10993-5. Finally, we have investigated the cytocompatibility of RSF films for corneal tissue engineering applications using SIRC cells (rabbit corneal cells). Alamar blue assay indicated >70 % cell viability in all the test samples with respect to cells cultured on TCPS. Subsequently, cytoskeletal staining and SEM analysis of cell laden test samples showed a good number of well adhered and well spread cells with typical corneal epithelial morphology (ovoid to cuboidal) on the test samples as compared to the control. Further, the cell laden test materials were visually observed and photographed and were found to be clear and optically transparent. Previously, Hazra et al 2016, Vazquez et al. 2017, Liu et al. 2010 and few others (Tran et al. 2018) have reported the compatibility of SF based biomaterials with corneal cells for corneal tissue engineering applications. Our results match with earlier reports, however, we also showed that the transparency remains unaltered even after cell culture studies.

Typically, process parameters would bring about conformational changes in SF which would in turn influence the material properties. In this study, fabrication processing parameters viz. solvent used (AQ, FA and HF) and post-fabrication processing parameters viz. methanol, steam and water annealing, were found to affect the topological, physical and degradation properties of SF films to a significant extent, however, the effects on chemical/ structural, optical and cytocompatibility properties were not evident in the current study. Based on the literature and our results, we postulate that SF changed from silk-I structure in reconstituted form to silk-II structure after film preparation and thereby influenced the material properties. However, additional details on secondary structure of SF could only reveal the relationship between structure and property of SF films. Further, molecular analysis of cells cultured on SF films could reveal effects of process parameters on cell – material interactions, if any.

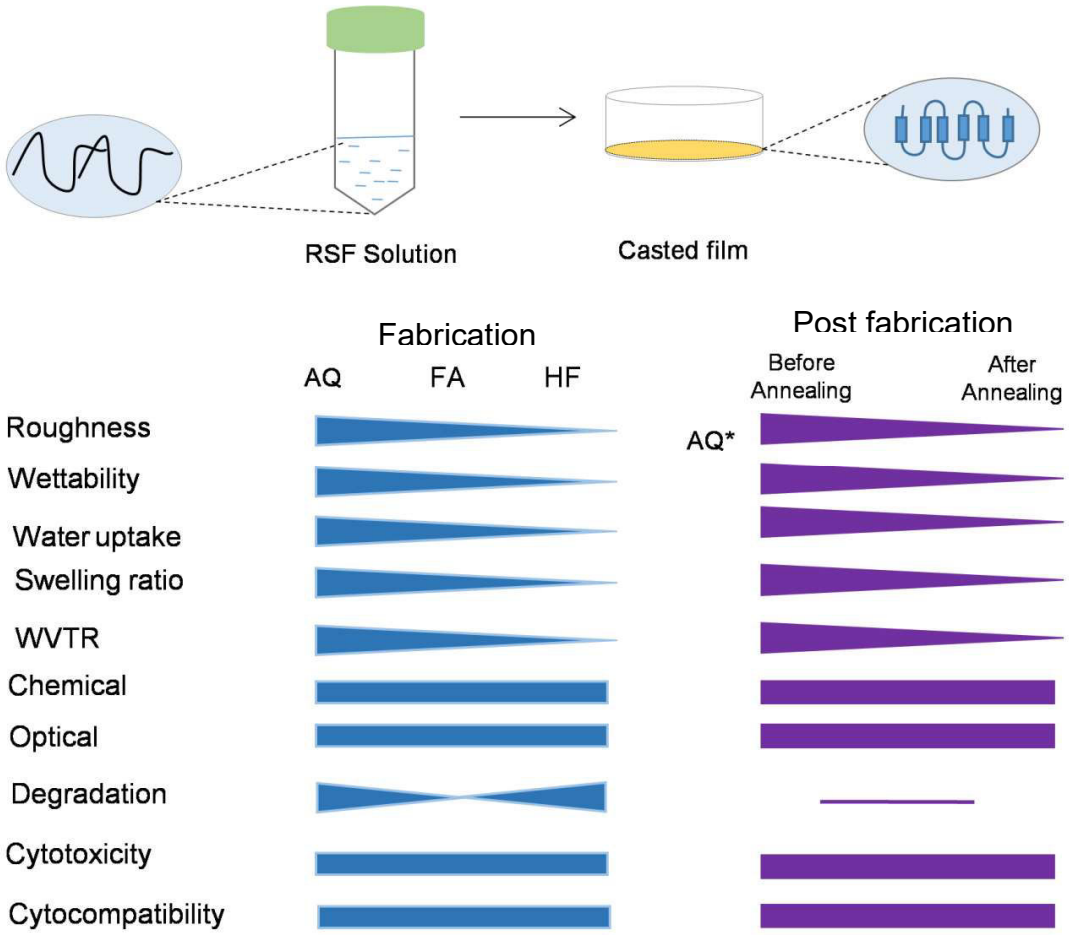

Figure 31. Insights into film preparation and bird-eye view of process - property relationship: Upon film preparation, SF changes from silk I (random structure) to silk II (highly organized structure). However, the process parameters used in the current study were found to influence the film properties to a great extent (notes: annealing related data was shown with respect to AQ films only; further, degradation was not performed for annealed samples).

Chapter 4: Conclusions and Future Prospects

4.1 Conclusions

With a hypothesis that various fabrication processes and post-fabrication processing in silk fibroin could influence the properties of silk fibroin derived films, we have (i) collected and degummed *Bombyx mori* silk cocoons into silk fibroin fibres and characterized its morphological and chemical/structural properties, (ii) reconstituted the degummed fibres into aqueous silk fibroin solution and characterized its molecular weight and chemical/structural properties, (iii) processed RSF solution in AQ, FA and HFIP into films by solvent casting approach, followed by annealing with methanol, water and steam, and characterized its morphological properties (SEM, surface roughness), physical properties (contact angle, swelling index, water uptake, WVT%), chemical/structural properties (FTIR), optical properties (optical clarity, absorbance spectra and transmission% in UV-Visible range), degradation properties, and finally (iv) evaluated its cytotoxicity with L929 cells and cytocompatibility with SIRC cells to determine its potential application in corneal tissue engineering.

Following are the conclusions of the current study:

1. The raw silk fibres were processed into silk fibroin fibres through degumming process. The yield% of degummed silk fibroin fibres was 68.6 ± 0.115 %. Morphological analysis by SEM revealed successful removal of sericin coating and calcium oxalate crystal deposits and subsequent reduction in fibre diameter from 25±3 μm to 10 ±3 μm. Further, elemental composition analysis by EDAX spectroscopy confirmed the successful removal of calcium oxalate crystals.
2. The degummed silk fibroin fibres were processed into reconstituted silk fibroin. Molecular weight analysis by SDS-PAGE showed a band >245 KDa indicating the H-chain (heavy chain) and faint low molecular bands at about 25 KDa indicating the L-chain (light chain) or P25 unit of silk fibroin protein. Further, chemical/structural analysis by ATR-FTIR showed characteristics peaks for amide I, II and III. Amide I peak shifted from 1620 cm^{-1}in DSF to 1640 cm^{-1}in RSF and therefore confirmed successful reconstitution of silk fibroin.
3. Subsequently RSF was made in AQ, FA and HF solutions and the films were obtained by solvent casting approach. They were then subjected to post-fabrication annealing process in methanol, water and steam. Morphological analysis by SEM revealed a decrease in roughness in the order of AQ > FA > HF. Further, surface profilometry

analysis showed decrease in root mean square roughness factor (Rq) in the same order of AQ (1.39)> FA (0.32) > HF (0.13). With respect to the effect of annealing on roughness factor, AQ, FA and HF films showed nearly50% reduction in roughness factor after annealing process in general. Thus, indicated process dependent differences in morphological and topographical properties of RSF films.

4. Contact angle increased in the order of AQ (73°) < FA (85°) < HF (89°) and thus indicated a decrease in surface wettability. Upon post-fabrication annealing, the contact angle was enhanced in AQ films, whereas in FA and HF films it was reduced. Water uptake and swelling ratio decreased in the order of AQ (57.6% and 1.58) > HF (27.3% and 1.22)> FA (28.3% and 1.14). Upon post-fabrication annealing, the swelling and water uptake was reduced. WVT% decreased in the order of AQ (35%) > FA (26%) > HF (23%). Upon post-fabrication annealing, permeability was enhanced.

5. Chemical/structural analysis of AQ, FA and HF films by ATR-FTIR showed characteristic peaks for amide I, II and III. In particular, amide I peak shifted from 1640 cm^{-1} in RSF to 1620 cm^{-1} in RSF films and therefore confirmed successful conformational change in structure from less ordered random coil to highly ordered beta sheet structure. Post fabrication annealing showed no changes in chemical/structural properties.

6. Visual observation of RSF films from all three solvents such as AQ, FA and HF, with and without annealing, showed excellent optical clarity. The optical clarity of RSF films in wet state also showed impressive optical clarity. Absorbance spectra (Vis range) of RSF films in dry state showed almost negligible absorbance, irrespective of fabrication and annealing process. After wetting, FA and HF derived films showed no changes, but, AQ films showed differential absorbance across various processing parameters. Similar trend was noticed for UVA range (350 nm), whereas negligible absorbance was recorded at UVC (250 nm) range and relatively high absorbance was recorded at UVB (300 nm) in all the films, both in dry and wet state.

7. As for transmission% all RSF films in dry state showed almost 80 – 90% transmission in visible range (500 nm), irrespective of fabrication and annealing process. After wetting, AQ, FA and HF derived films showed no noticeable changes in the overall spectral pattern, across various processing parameters. Transmission% in UVC (250 nm) range was 60 – 80% and decreased by 2-fold after annealing, in UVB (300 nm) range it was 20 – 40% and decreased by 3.5-fold, and in UVA (350 nm) range it was

70 – 80% and decreased by 1.5-fold. Transmittance % of films after incubation in STF for 4 weeks was analysed. All the films (with and without annealing) showed about 90% transmission in visible range and there was no significant difference in transmission% even after 4 weeks of incubation in STF.

8. The silk films were analysed for degradation profile till 28 days in PBS, STF and ENZ. Weight loss % was higher in AQ films incubated in ENZ (72%) compared to PBS (12%) and STF (4%). Similarly, HF films degraded more in ENZ (86%), compared to PBS (5%) and STF (5%). Whereas FA films exhibited only about 12% weight loss in ENZ, that was close to 7% in PBS and 7.5% STF at week 4.
9. Test on extract-based cytotoxicity assay as per ISO 10993-5 using L929 cell line, indicated that the test samples (AQ, FA and HF with and without annealing) were non-cytotoxic (grade 0), like that of cell control. Subsequent MTT assay showed about 80-100 % cell viability in the test samples (AQ, FA and HF with and without annealing), close to that of 100 % cell viability in cell control.
10. Finally, we have cultured SIRC cells (rabbit corneal cells) on RSF films and determined cell viability and cell adhesion with respect to cells cultured on TCPS (tissue culture polystyrene dish). Alamar blue assay indicated>70 % cell viability in all the test samples with respect to cells cultured on TCPS. Subsequently, cytoskeletal staining and SEM analysis of cell laden test samples collectively showed a good number of well adhered and well spread cells with typical corneal epithelial morphology (ovoid to cuboidal) on the test samples as compared to the control. Further, the cell laden test materials were visually observed and photographed and were found to be clear and optically transparent.

Overall, we have successfully demonstrated degumming of raw cocoons, reconstitution of silk fibroin, and preparation of films by solvent casting with different fabrication and post fabrication processing conditions. We found process dependent differences in morpho-topological, physico-chemical, optical and biodegradation properties of RSF films. We found that the RSF films, irrespective of processing conditions, were non-cytotoxic. Finally, RSF films, prepared by different processing conditions, were found to be compatible with corneal cells and therefore have to be more explored for potential application in corneal tissue engineering.

4.2 Future prospects

The current study was the first of its kind to determine the effects of process parameters on silk fibroin films in the context of corneal tissue engineering. However, this was a pilot study to seek insights into various morpho-topological, physico-chemical, and preliminary biological properties. There is scope for further research on this topic to take the concept from bench to bed side. Following are few areas to focus in future:

1. In this study, we have not focused on pre-fabrication processing of silk i.e. degumming and aqueous reconstitution (parameters: type of chemical, concentration of chemical, time and temperature). However, these are also reported to be critical parameters that influence subsequent material properties, and therefore could be studied in the context of corneal tissue engineering.
2. In this study, during solvent casting of film, we have varied the type of solvent used but kept all other parameters constant (polymer concentration, temperature and time). These parameters could also influence the subsequent material properties, and therefore could be studied in the context of corneal tissue engineering.
3. In terms of post-fabrication processing i.e. annealing, we have used three methods - methanol, water and steam in vapour form. However, there were other means of annealing as reported in literature, which could be studied to see the effects on material properties in the context of corneal tissue engineering.
4. In the current, we have not performed mechanical testing; however, we believe a future study on this aspect could reveal interesting process property relationship. As for degradation, we have considered AQ, FA and HF films without annealing. We believe that a study on AQ, FA and HF annealed samples should be taken up to determine the rate of degradation upon annealing.
5. Corneal cell culture study could be extended to a long-term period of 4 weeks including air liquid interface mode of culture in order to obtain a corneal epithelial/ stromal equivalent having tissue histology close to nature. Further, a molecular analysis of cell material interactions could provide useful insights.

Subsequently, based on the inputs from this and above-mentioned futuristic studies, silk fibroin films with appropriate properties could be evaluated *in vivo* for potential applications in corneal tissue engineering.

References

Aigner, Tamara Bernadette, Elise DeSimone, and Thomas Scheibel. 2018. "Biomedical Applications of Recombinant Silk-Based Materials." *Advanced Materials* 30 (19): 1704636. https://doi.org/10.1002/adma.201704636.

Akturk, Omer, Kemal Kismet, Ahmet C. Yasti, Serdar Kuru, Mehmet E. Duymus, Feridun Kaya, Muzaffer Caydere, Sema Hucumenoglu, and Dilek Keskin. 2016. "Wet Electrospun Silk Fibroin/Gold Nanoparticle 3D Matrices for Wound Healing Applications." *RSC Advances* 6 (16): 13234–50. https://doi.org/10.1039/C5RA24225H.

Altman, Gregory H, Frank Diaz, Caroline Jakuba, Tara Calabro, Rebecca L Horan, Jingsong Chen, Helen Lu, John Richmond, and David L Kaplan. 2003. "Silk-Based Biomaterials." *Biomaterials* 24 (3): 401–16. https://doi.org/10.1016/S0142-9612(02)00353-8.

Applegate, Matthew B., Benjamin P. Partlow, Jeannine Coburn, Benedetto Marelli, Christopher Pirie, Roberto Pineda, David L. Kaplan, and Fiorenzo G. Omenetto. 2016. "Photocrosslinking of Silk Fibroin Using Riboflavin for Ocular Prostheses." *Advanced Materials* 28 (12): 2417–20. https://doi.org/10.1002/adma.201504527.

Asadian, Mahtab, Ke Vin Chan, Mohammad Norouzi, Silvia Grande, Pieter Cools, Rino Morent, and Nathalie De Geyter. 2020. "Fabrication and Plasma Modification of Nanofibrous Tissue Engineering Scaffolds." *Nanomaterials* 10 (1): 119. https://doi.org/10.3390/nano10010119.

Barbosa, Nilseia, Luiz da Rosa, Artur Menezes, Juraci Reis, Alessandro Facure, and Delson Braz. 2014. "Assessment of Ocular Beta Radiation Dose Distribution Due to 106Ru/106Rh Brachytherapy Applicators Using MCNPX Monte Carlo Code." *International Journal of Cancer Therapy and Oncology* 2 (3): 02038. https://doi.org/10.14319/ijcto.0203.8.

Beebe, David C., and J.Michael Coats. 2000. "The Lens Organizes the Anterior Segment: Specification of Neural Crest Cell Differentiation in the Avian Eye." *Developmental Biology* 220 (2): 424–31. https://doi.org/10.1006/dbio.2000.9638.

Boote, Craig, Sally Dennis, Richard H. Newton, Hina Puri, and Keith M. Meek. 2003. "Collagen Fibrils Appear More Closely Packed in the Prepupillary Cornea: Optical and Biomechanical Implications." *Investigative Opthalmology & Visual Science* 44 (7): 2941. https://doi.org/10.1167/iovs.03-0131.

Boulet-Audet, Maxime, Chris Holland, Tom Gheysens, and Fritz Vollrath. 2016. "Dry-Spun Silk Produces Native-Like Fibroin Solutions." *Biomacromolecules* 17 (10): 3198–3204. https://doi.org/10.1021/acs.biomac.6b00887.

Bray, Laura J., Karina A. George, S. Louise Ainscough, Dietmar W. Hutmacher, Traian V. Chirila, and Damien G. Harkin. 2011. "Human Corneal Epithelial Equivalents Constructed on *Bombyx mori* Silk Fibroin Membranes." *Biomaterials* 32 (22): 5086–91. https://doi.org/10.1016/j.biomaterials.2011.03.068.

Cai, Kaiyong, Kangde Yao, Songbai Lin, Zhiming Yang, Xiuqiong Li, Huiqi Xie, Tingwu Qing, and Laibao Gao. 2002. "Poly(d,l-Lactic Acid) Surfaces Modified by Silk Fibroin: Effects on the Culture of Osteoblast *in vitro*." *Biomaterials* 23 (4): 1153–60. https://doi.org/10.1016/S0142-9612(01)00230-7.

Chen, Jingsong, Gregory H. Altman, Vassilis Karageorgiou, Rebecca Horan, Adam Collette, Vladimir Volloch, Tara Colabro, and David L. Kaplan. 2003. "Human Bone Marrow Stromal Cell and Ligament Fibroblast Responses on RGD-Modified Silk Fibers." *Journal of Biomedical Materials Research* 67A (2): 559–70. https://doi.org/10.1002/jbm.a.10120.

Christopher T. Hood, Ayad A. Farjo. n.d. "Corneal Anatomy,Physiology,and Wound Healing." In *Corneal Anatomy,Physiology,and Wound Healing*. Vol. part 4. Myron Yanoff, Jay S Duker.

Chung, Da Eun, et al. "Effects of Different Bombyx mori Silkworm Varieties on the Structural Characteristics and Properties of Silk." *International Journal of Biological Macromolecules*, vol. 79, Aug. 2015, pp. 943–51. DOI.org (Crossref), doi:10.1016/j.ijbiomac.2015.06.012.

Cirillo, B., M. Morra, and G. Catapano. 2004. "Adhesion and Function of Rat Liver Cells Adherent to Silk Fibroin/Collagen Blend Films." *The International Journal of Artificial Organs* 27 (1): 60–68. https://doi.org/10.1177/039139880402700112.

Dal Pra, Ilaria, Anna Chiarini, Alessandra Boschi, Giuliano Freddi, and Ubaldo Armato. 2006. "Novel Dermo-Epidermal Equivalents on Silk Fibroin-Based Formic Acid-Crosslinked Three-Dimensional Nonwoven Devices with Prospective Applications in Human Tissue Engineering/Regeneration/Repair." *International Journal of Molecular Medicine*, August. https://doi.org/10.3892/ijmm.18.2.241.

Das, Suradip, Manav Sharma, Dhiren Saharia, Kushal Konwar Sarma, Monalisa Goswami Sarma, Bibhuti Bhusan Borthakur, and Utpal Bora. 2015. "*In vivo* Studies of Silk Based Gold Nano-Composite Conduits for Functional Peripheral Nerve Regeneration." *Biomaterials* 62 (September): 66–75. https://doi.org/10.1016/j.biomaterials.2015.04.047.

DelMonte, Derek W., and Terry Kim. 2011. "Anatomy and Physiology of the Cornea:" *Journal of Cataract & Refractive Surgery* 37 (3): 588–98. https://doi.org/10.1016/j.jcrs.2010.12.037.

Dong, Yixuan, Pin Dong, Di Huang, Liling Mei, Yaowen Xia, Zhouhua Wang, Xin Pan, Ge Li, and Chuanbin Wu. 2015. "Fabrication and Characterization of Silk Fibroin-Coated Liposomes for Ocular Drug Delivery." *European Journal of Pharmaceutics and Biopharmaceutics* 91 (April): 82–90. https://doi.org/10.1016/j.ejpb.2015.01.018.

Ebrahimi, Davoud, Olena Tokareva, Nae Gyune Rim, Joyce Y. Wong, David L. Kaplan, and Markus J. Buehler. 2015. "Silk–Its Mysteries, How It Is Made, and How It Is Used." *ACS Biomaterials Science & Engineering* 1 (10): 864–76. https://doi.org/10.1021/acsbiomaterials.5b00152.

Eghrari, Allen O., S. Amer Riazuddin, and John D. Gottsch. 2015. "Overview of the Cornea." In *Progress in Molecular Biology and Translational Science*, 134:7–23. Elsevier. https://doi.org/10.1016/bs.pmbts.2015.04.001.

Galler, Kerstin M, and Rena N D'Souza. 2011. "Tissue Engineering Approaches for Regenerative Dentistry." *Regenerative Medicine* 6 (1): 111–24. https://doi.org/10.2217/rme.10.86.

Gotoh, Y. 2004. "Preparation of Lactose–Silk Fibroin Conjugates and Their Application as a Scaffold for Hepatocyte Attachment." *Biomaterials* 25 (6): 1131–40. https://doi.org/10.1016/S0142-9612(03)00633-1.

Gotoh, Yohko, Yasuyuki Ishizuka, Tomokazu Matsuura, and Shingo Niimi. 2011. "Spheroid Formation and Expression of Liver-Specific Functions of Human Hepatocellular Carcinoma-Derived FLC-4 Cells Cultured in Lactose−Silk Fibroin Conjugate Sponges." *Biomacromolecules* 12 (5): 1532–39. https://doi.org/10.1021/bm101495c.

Ha, Sung-Won, Alan E. Tonelli, and Samuel M. Hudson. 2005. "Structural Studies of *BombyxmOri* Silk Fibroin during Regeneration from Solutions and Wet Fiber Spinning." *Biomacromolecules* 6 (3): 1722–31. https://doi.org/10.1021/bm050010y.

Hakimi, Osnat, David P. Knight, Fritz Vollrath, and Pankaj Vadgama. 2007. "Spider and Mulberry Silkworm Silks as Compatible Biomaterials." *Composites Part B: Engineering* 38 (3): 324–37. https://doi.org/10.1016/j.compositesb.2006.06.012.

Hanna, C., D. S. Bicknell, and J. E. O'Brien. 1961. "Cell Turnover in the Adult Human Eye." *Archives of Ophthalmology* 65 (5): 695–98. https://doi.org/10.1001/archopht.1961.01840020697016.

Hazra, Sarbani, Sudip Nandi, Deboki Naskar, Rajdeep Guha, Sushovan Chowdhury, Nirparaj Pradhan, Subhas C. Kundu, and Aditya Konar. 2016. "Non-Mulberry Silk Fibroin Biomaterial for Corneal Regeneration." *Scientific Reports* 6 (1): 21840. https://doi.org/10.1038/srep21840.

Huang, Guoping, Danfeng Yang, Chunfeng Sun, Jianping Huang, Keping Chen, Chunxia Zhang, Huiqing Chen, and Qin Yao. 2014. "A Quicker Degradation Rate Is Yielded by a Novel Kind of Transgenic Silk Fibroin Consisting of Shortened Silk Fibroin Heavy Chains Fused with Matrix Metalloproteinase

Cleavage Sites." *Journal of Materials Science: Materials in Medicine* 25 (8): 1833–42. https://doi.org/10.1007/s10856-014-5220-6.

Huang, Xiangyu, Suna Fan, Alhadi Ibrahim Mohammed Altayp, Yaopeng Zhang, Huili Shao, Xuechao Hu, Minkai Xie, and Yuemin Xu. 2014. "Tunable Structures and Properties of Electrospun Regenerated Silk Fibroin Mats Annealed in Water Vapor at Different Times and Temperatures." *Journal of Nanomaterials* 2014: 1–7. https://doi.org/10.1155/2014/682563.

Inoue, Satoshi, Kazunori Tanaka, Fumio Arisaka, Sumiko Kimura, Kohei Ohtomo, and Shigeki Mizuno. 2000. "Silk Fibroin of *Bombyx mori* Is Secreted, Assembling a High Molecular Mass Elementary Unit Consisting of H-Chain, L-Chain, and P25, with a 6:6:1 Molar Ratio." *Journal of Biological Chemistry* 275 (51): 40517–28. https://doi.org/10.1074/jbc.M006897200.

Jaramillo-Quiceno, Natalia, Catalina Álvarez-López, and Adriana Restrepo-Osorio. 2017. "Structural and Thermal Properties of Silk Fibroin Films Obtained from Cocoon and Waste Silk Fibers as Raw Materials." *Procedia Engineering* 200: 384–88. https://doi.org/10.1016/j.proeng.2017.07.054.

Jester, J.V., T. Moller-Pedersen, J. Huang, C.M. Sax, W.T. Kays, H.D. Cavangh, W.M. Petroll, and J. Piatigorsky. 1999. "The Cellular Basis of Corneal Transparency: Evidence for 'Corneal Crystallins.'" *Journal of Cell Science* 112 (5): 613.

Jin, Hyoung-Joon, Jaehyung Park, Regina Valluzzi, Peggy Cebe, and David L. Kaplan. 2004. "Biomaterial Films of *BombyxMOri* Silk Fibroin with Poly(Ethylene Oxide)." *Biomacromolecules* 5 (3): 711–17. https://doi.org/10.1021/bm0343287.

Kaewpirom, Supranee, and Siridech Boonsang. 2020. "Influence of Alcohol Treatments on Properties of Silk-Fibroin-Based Films for Highly Optically Transparent Coating Applications." *RSC Advances* 10 (27): 15913–23. https://doi.org/10.1039/D0RA02634D.

Kasoju, Naresh, and Utpal Bora. 2012a. "Silk Fibroin in Tissue Engineering." *Advanced Healthcare Materials* 1 (4): 393–412. https://doi.org/10.1002/adhm.201200097.

"Silk Fibroin Based Biomimetic Artificial Extracellular Matrix for Hepatic Tissue Engineering Applications." *Biomedical Materials* 7 (4): 045004. https://doi.org/10.1088/1748-6041/7/4/045004.

Kasoju, Naresh, Nicholas Hawkins, Ognen Pop-Georgievski, Dana Kubies, and Fritz Vollrath. 2016. "Silk Fibroin Gelation via Non-Solvent Induced Phase Separation." *Biomaterials Science* 4 (3): 460–73. https://doi.org/10.1039/C5BM00471C.

Kaur, Jasjeet, Rangam Rajkhowa, Takuya Tsuzuki, and Xungai Wang. 2015. "Crystals in Antheraea Assamensis Silkworm Cocoon: Their Removal, Recovery and Roles." *Materials & Design* 88 (December): 236–44. https://doi.org/10.1016/j.matdes.2015.08.148.

Keten, Sinan, and Markus J. Buehler. 2010. "Atomistic Model of the Spider Silk Nanostructure." *Applied Physics Letters* 96 (15): 153701. https://doi.org/10.1063/1.3385388.

Koh, Leng-Duei, Yuan Cheng, Choon-Peng Teng, Yin-Win Khin, Xian-Jun Loh, Si-Yin Tee, Michelle Low, et al. 2015. "Structures, Mechanical Properties and Applications of Silk Fibroin Materials." *Progress in Polymer Science* 46 (July): 86–110. https://doi.org/10.1016/j.progpolymsci.2015.02.001.

Kong, Bin, and Shengli Mi. 2016. "Electrospun Scaffolds for Corneal Tissue Engineering: A Review." *Materials* 9 (8): 614. https://doi.org/10.3390/ma9080614.

Kumar, Nupur, Heer Joisher, and Anasuya Ganguly. 2017. "Polymeric Scaffolds for Pancreatic Tissue Engineering: A Review." *The Review of Diabetic Studies* 14 (4): 334–53. https://doi.org/10.1900/RDS.2017.14.334.

Kumar, Sandeep, and Sandeep Kumar Singh. 2017. "Fabrication and Characterization of Fibroin Solution and Nanoparticle from Silk Fibers of *Bombyx mori*." *Particulate Science and Technology* 35 (3): 304–13. https://doi.org/10.1080/02726351.2016.1154908.

Lagali, Neil, Johan Germundsson, and Per Fagerholm. 2009. "The Role of Bowman's Layer in Corneal Regeneration after Phototherapeutic Keratectomy: A Prospective Study Using *In vivo* Confocal Microscopy." *Investigative Opthalmology & Visual Science* 50 (9): 4192. https://doi.org/10.1167/iovs.09-3781.

Langer, R, and J. Vacanti. 1993. "Tissue Engineering." *Science* 260 (5110): 920–26. https://doi.org/10.1126/science.8493529.

Lawrence, Brian D., Scott Wharram, Jonathan A. Kluge, Gary G. Leisk, Fiorenzo G. Omenetto, Mark I. Rosenblatt, and David L. Kaplan. 2010. "Effect of Hydration on Silk Film Material Properties: Effect of Hydration on Silk Film Material Properties." *Macromolecular Bioscience* 10 (4): 393–403. https://doi.org/10.1002/mabi.200900294.

Levin, Brett, Rangam Rajkhowa, Sharon Leanne Redmond, and Marcus David Atlas. 2009. "Grafts in Myringoplasty: Utilizing a Silk Fibroin Scaffold as a Novel Device." *Expert Review of Medical Devices* 6 (6): 653–64. https://doi.org/10.1586/erd.09.47.

Levin, Brett, Sharon Leanne Redmond, Rangam Rajkhowa, Robert Henry Eikelboom, Robert Jeffery Marano, and Marcus David Atlas. 2010. "Preliminary Results of the Application of a Silk Fibroin Scaffold to Otology." *Otolaryngology–Head and Neck Surgery* 142 (3_suppl): S33–35. https://doi.org/10.1016/j.otohns.2009.06.746.

Levin, L.A., S.F.E. Nilsson, J.V. Hoeve, S. Wu, P.L. Kaufman, and A. Alm. 2011. *Adler's Physiology of the Eye E-Book*. Elsevier Health Sciences. https://books.google.co.in/books?id=r1BtVqwSJBsC.

Li, Gang, Yi Li, Guoqiang Chen, Jihuan He, Yifan Han, Xiaoqin Wang, and David L. Kaplan. 2015. "Silk-Based Biomaterials in Biomedical Textiles and Fiber-Based Implants." *Advanced Healthcare Materials* 4 (8): 1134–51. https://doi.org/10.1002/adhm.201500002.

Li, Zi-Heng, Shi-Chen Ji, Ya-Zhen Wang, Xing-Can Shen, and Hong Liang. 2013a. "Silk Fibroin-Based Scaffolds for Tissue Engineering." *Frontiers of Materials Science* 7 (3): 237–47. https://doi.org/10.1007/s11706-013-0214-8.

"Silk Fibroin-Based Scaffolds for Tissue Engineering." *Frontiers of Materials Science* 7 (3): 237–47. https://doi.org/10.1007/s11706-013-0214-8.

Liu, Jian, Huijuan Chen, Yongfeng Wang, Gang Li, Zhaozhu Zheng, David L. Kaplan, Xiuli Wang, and Xiaoqin Wang. 2020. "Flexible Water-Absorbing Silk-Fibroin Biomaterial Sponges with Unique Pore Structure for Tissue Engineering." *ACS Biomaterials Science & Engineering* 6 (3): 1641–49. https://doi.org/10.1021/acsbiomaterials.9b01721.

Liu, Jingbo, Brian D. Lawrence, Aihong Liu, Ivan R. Schwab, Lauro A. Oliveira, and Mark I. Rosenblatt. 2012. "Silk Fibroin as a Biomaterial Substrate for Corneal Epithelial Cell Sheet Generation." *Investigative Opthalmology & Visual Science* 53 (7): 4130. https://doi.org/10.1167/iovs.12-9876.

Liu, Qichun, Fang Wang, Zhenggui Gu, Qingyu Ma, and Xiao Hu. 2018. "Exploring the Structural Transformation Mechanism of Chinese and Thailand Silk Fibroin Fibers and Formic-Acid Fabricated Silk Films." *International Journal of Molecular Sciences* 19 (11): 3309. https://doi.org/10.3390/ijms19113309.

Liu, Tie-lian, Jing-cheng Miao, Wei-hua Sheng, Yu-feng Xie, Quan Huang, Yun-bo Shan, and Ji-cheng Yang. 2010. "Cytocompatibility of Regenerated Silk Fibroin Film: A Medical Biomaterial Applicable to Wound Healing." *Journal of Zhejiang University SCIENCE B* 11 (1): 10–16. https://doi.org/10.1631/jzus.B0900163.

Lu, Qiang, Xiao Hu, Xiaoqin Wang, Jonathan A. Kluge, Shenzhou Lu, Peggy Cebe, and David L. Kaplan. 2010. "Water-Insoluble Silk Films with Silk I Structure." *Acta Biomaterialia* 6 (4): 1380–87. https://doi.org/10.1016/j.actbio.2009.10.041.

Luangbudnark, Witoo, Jarupa Viyoch, Wiroon Laupattarakasem, Palakorn Surakunprapha, and Pisamai Laupattarakasem. 2012. "Properties and Biocompatibility of Chitosan and Silk Fibroin Blend Films

for Application in Skin Tissue Engineering." *The Scientific World Journal* 2012: 1–10. https://doi.org/10.1100/2012/697201.

Ma, Buyong, and Ruth Nussinov. 2009. "Molecular Dynamics Simulations of Alanine Rich β-Sheet Oligomers: Insight into Amyloid Formation." *Protein Science* 11 (10): 2335–50. https://doi.org/10.1110/ps.4270102.

Madden, Peter W., Jonathan N.X. Lai, Karina A. George, Talia Giovenco, Damien G. Harkin, and Traian V. Chirila. 2011. "Human Corneal Endothelial Cell Growth on a Silk Fibroin Membrane." *Biomaterials* 32 (17): 4076–84. https://doi.org/10.1016/j.biomaterials.2010.12.034.

Madduri, Srinivas, Pietro di Summa, Michaël Papaloïzos, Daniel Kalbermatten, and Bruno Gander. 2010. "Effect of Controlled Co-Delivery of Synergistic Neurotrophic Factors on Early Nerve Regeneration in Rats." *Biomaterials* 31 (32): 8402–9. https://doi.org/10.1016/j.biomaterials.2010.07.052.

Mane, Pramod C., Manish D. Shinde, Sanjana Varma, Bhushan P. Chaudhari, Amanullah Fatehmulla, M. Shahabuddin, Dinesh P. Amalnerkar, Abdullah M. Aldhafiri, and Ravindra D. Chaudhari. 2020. "Highly Sensitive Label-Free Bio-Interfacial Colorimetric Sensor Based on Silk Fibroin-Gold Nanocomposite for Facile Detection of Chlorpyrifos Pesticide." *Scientific Reports* 10 (1): 4198. https://doi.org/10.1038/s41598-020-61130-y.

Martin, Ivan, David Wendt, and Michael Heberer. 2004. "The Role of Bioreactors in Tissue Engineering." *Trends in Biotechnology* 22 (2): 80–86. https://doi.org/10.1016/j.tibtech.2003.12.001.

McGill, Meghan, Gregory P. Holland, and David L. Kaplan. 2019. "Experimental Methods for Characterizing the Secondary Structure and Thermal Properties of Silk Proteins." *Macromolecular Rapid Communications* 40 (1): 1800390. https://doi.org/10.1002/marc.201800390.

Meinel, Lorenz, Sandra Hofmann, Oliver Betz, Robert Fajardo, Hans P. Merkle, Robert Langer, Christopher H. Evans, Gordana Vunjak-Novakovic, and David L. Kaplan. 2006. "Osteogenesis by Human Mesenchymal Stem Cells Cultured on Silk Biomaterials: Comparison of Adenovirus Mediated Gene Transfer and Protein Delivery of BMP-2." *Biomaterials* 27 (28): 4993–5002. https://doi.org/10.1016/j.biomaterials.2006.05.021.

Melke, Johanna, Swati Midha, Sourabh Ghosh, Keita Ito, and Sandra Hofmann. 2016. "Silk Fibroin as Biomaterial for Bone Tissue Engineering." *Acta Biomaterialia* 31 (February): 1–16. https://doi.org/10.1016/j.actbio.2015.09.005.

Min, Byung-Moo, Gene Lee, So Hyun Kim, Young Sik Nam, Taek Seung Lee, and Won Ho Park. 2004. "Electrospinning of Silk Fibroin Nanofibers and Its Effect on the Adhesion and Spreading of Normal Human Keratinocytes and Fibroblasts *in vitro*." *Biomaterials* 25 (7–8): 1289–97. https://doi.org/10.1016/j.biomaterials.2003.08.045.

Mobaraki, Mohammadmahdi, Reza Abbasi, Sajjad Omidian Vandchali, Maryam Ghaffari, Fathollah Moztarzadeh, and Masoud Mozafari. 2019. "Corneal Repair and Regeneration: Current Concepts and Future Directions." *Frontiers in Bioengineering and Biotechnology* 7 (June): 135. https://doi.org/10.3389/fbioe.2019.00135.

Mondal, m., k. Trivedy, and s. Nirmal kumar. 2007. "the silk proteins, sericin and fibroin in silkworm, *Bombyx mori* linn., - a review." *Caspian journal of environmental sciences (cjes)* 5 (2): 63–76.

Mousumi Mondal, Kanika Trivedy , S. Nirmal Kumar and Vineet Kumar. 2007. "Scanning Electron Microscopic Study on the Cross Sections of Cocoon Filament and Degummed Fiber of Different Breeds/Hybrids of Mulberry Silkworm, *Bombyx mori*." *Journal of Entomology* 4: 362–70.

Nguyen, Thang Phan, Quang Vinh Nguyen, Van-Huy Nguyen, Thu-Ha Le, Vu Quynh Nga Huynh, Dai-Viet N. Vo, Quang Thang Trinh, Soo Young Kim, and Quyet Van Le. 2019a. "Silk Fibroin-Based Biomaterials for Biomedical Applications: A Review." *Polymers* 11 (12): 1933. https://doi.org/10.3390/polym11121933.

"Silk Fibroin-Based Biomaterials for Biomedical Applications: A Review." *Polymers* 11 (12): 1933. https://doi.org/10.3390/polym11121933.

O'Brien, Fergal J. 2011. "Biomaterials & Scaffolds for Tissue Engineering." *Materials Today* 14 (3): 88–95. https://doi.org/10.1016/S1369-7021(11)70058-X.

Peh, Gary S. L., Roger W. Beuerman, Alan Colman, Donald T. Tan, and Jodhbir S. Mehta. 2011. "Human Corneal Endothelial Cell Expansion for Corneal Endothelium Transplantation: An Overview:" *Transplantation* 91 (8): 811–19. https://doi.org/10.1097/TP.0b013e3182111f01.

Polse, K A, R J Brand, S R Cohen, and M Guillon. 1990. "Hypoxic Effects on Corneal Morphology and Function." *Investigative Ophthalmology & Visual Science* 31 (8): 1542–54.

Qi, Ning, Bing Zhao, Shu-Dong Wang, Salem S. Al-Deyab, and Ke-Qin Zhang. 2015. "Highly Flexible and Conductive Composite Films of Silk Fibroin and Silver Nanowires for Optoelectronic Devices." *RSC Advances* 5 (63): 50878–82. https://doi.org/10.1039/C5RA03501E.

Qi, Yu, Hui Wang, Kai Wei, Ya Yang, Ru-Yue Zheng, Ick Kim, and Ke-Qin Zhang. 2017. "A Review of Structure Construction of Silk Fibroin Biomaterials from Single Structures to Multi-Level Structures." *International Journal of Molecular Sciences* 18 (3): 237. https://doi.org/10.3390/ijms18030237.

Ramachandran, Charanya, Prerak Gupta, Swatilekha Hazra, and Biman B. Mandal. 2020. "*In vitro* Culture of Human Corneal Endothelium on Non-Mulberry Silk Fibroin Films for Tissue Regeneration." *Translational Vision Science & Technology* 9 (4): 12. https://doi.org/10.1167/tvst.9.4.12.

Ren, Yong-Juan, Zi-You Zhou, Bing-Fang Liu, Qun-Yuan Xu, and Fu-Zhai Cui. 2009. "Preparation and Characterization of Fibroin/Hyaluronic Acid Composite Scaffold." *International Journal of Biological Macromolecules* 44 (4): 372–78. https://doi.org/10.1016/j.ijbiomac.2009.02.004.

Rockwood, Danielle N, Rucsanda C Preda, Tuna Yücel, Xiaoqin Wang, Michael L Lovett, and David L Kaplan. 2011. "Materials Fabrication from *Bombyx mori* Silk Fibroin." *Nature Protocols* 6 (10): 1612–31. https://doi.org/10.1038/nprot.2011.379.

Rowsey, Tyler G., and Dimitrios Karamichos. 2017. "The Role of Lipids in Corneal Diseases and Dystrophies: A Systematic Review." *Clinical and Translational Medicine* 6 (1): 30. https://doi.org/10.1186/s40169-017-0158-1.

Schmidt, Christine E., and Jennie Baier Leach. 2003. "Neural Tissue Engineering: Strategies for Repair and Regeneration." *Annual Review of Biomedical Engineering* 5 (1): 293–347. https://doi.org/10.1146/annurev.bioeng.5.011303.120731.

"SDS-PAGE for Protein Electrophoresis." 2016. iGEM Stockholm.

Shah, Ajay, Jamie Brugnano, Stacy Sun, Ajoy Vase, and Elizabeth Orwin. 2008a. "The Development of a Tissue-Engineered Cornea: Biomaterials and Culture Methods." *Pediatric Research* 63 (5): 535–44. https://doi.org/10.1203/PDR.0b013e31816bdf54.

"The Development of a Tissue-Engineered Cornea: Biomaterials and Culture Methods." *Pediatric Research* 63 2018 (5): 535–44. https://doi.org/10.1203/PDR.0b013e31816bdf54.

Sommer, A., and Muhilal. 1982. "Nutritional Factors in Corneal Xerophthalmia and Keratomalacia." *Archives of Ophthalmology* 100 (3): 399–403. https://doi.org/10.1001/archopht.1982.01030030401002.

Song, Jeong Eun, Bo Ra Sim, Yoo Shin Jeon, Han Sol Kim, Eun Yeong Shin, Cristiano Carlomagno, and Gilson Khang. 2019a. "Characterization of Surface Modified Glycerol/Silk Fibroin Film for Application to Corneal Endothelial Cell Regeneration." *Journal of Biomaterials Science, Polymer Edition* 30 (4): 263–75. https://doi.org/10.1080/09205063.2018.1535819.

"Characterization of Surface Modified Glycerol/Silk Fibroin Film for Application to Corneal Endothelial Cell Regeneration." 2019 *Journal of Biomaterials Science, Polymer Edition* 30 (4): 263–75. https://doi.org/10.1080/09205063.2018.1535819.

Sridhar, Mittanamalli S. 2018. “Anatomy of Cornea and Ocular Surface.” *Indian Journal of Ophthalmology* 66 (2): 190–94. https://doi.org/10.4103/ijo.IJO_646_17.

Stiemke, Monicka M., Henry F. Edelhauser, and Dayle H. Geroski. 1991. “The Developing Corneal Endothelium: Correlation of Morphology, Hydration and Na/K ATPase Pump Site Density.” *Current Eye Research* 10 (2): 145–56. https://doi.org/10.3109/02713689109001742.

Tamada, Yasushi. 2005. “New Process to Form a Silk Fibroin Porous 3-D Structure.” *Biomacromolecules* 6 (6): 3100–3106. https://doi.org/10.1021/bm050431f.

Tanaka, Kazunori, Naoki Kajiyama, Kiyohide Ishikura, Shou Waga, Aiko Kikuchi, Kohei Ohtomo, Takashi Takagi, and Shigeki Mizuno. 1999. “Determination of the Site of Disulfide Linkage between Heavy and Light Chains of Silk Fibroin Produced by *Bombyx mori*.” *Biochimica et Biophysica Acta (BBA) - Protein Structure and Molecular Enzymology* 1432 (1): 92–103. https://doi.org/10.1016/S0167-4838(99)00088-6.

Teh, Thomas K H, Siew-Lok Toh, and James C H Goh. 2010. “Optimization of the Silk Scaffold Sericin Removal Process for Retention of Silk Fibroin Protein Structure and Mechanical Properties.” *Biomedical Materials* 5 (3): 035008. https://doi.org/10.1088/1748-6041/5/3/035008.

Tran, Simon H., Clive G. Wilson, and F. Philipp Seib. 2018. “A Review of the Emerging Role of Silk for the Treatment of the Eye.” *Pharmaceutical Research* 35 (12): 248. https://doi.org/10.1007/s11095-018-2534-y.

Tsubouchi, Kozo, Hiroshi Nakao, Yumiko Igarashi, Yoko Takasu, and Hiromi Yamada. 2003. “*Bombyx mori* Fibroin Enhanced the Proliferation of Cultured Human Skin Fibroblasts.” *Journal of Insect Biotechnology and Sericology* 72 (1): 65–69. https://doi.org/10.11416/jibs.72.65.

Umemoto, Terumasa, Masayuki Yamato, Kohji Nishida, and Teruo Okano. 2013. “Regenerative Medicine of Cornea by Cell Sheet Engineering Using Temperature-Responsive Culture Surfaces.” *Chinese Science Bulletin* 58 (35): 4349–56. https://doi.org/10.1007/s11434-013-5742-1.

V. Kearns A. Crawford. 2008. “Silk-Based Biomaterials for Tissue Engineering.” N Ashammakhi, R Reis, & F Chiellini.

Vashist, Praveen, Noopur Gupta, Radhika Tandon, SanjeevK Gupta, and V Sreenivas. 2013. “Burden of Corneal Blindness in India.” *Indian Journal of Community Medicine* 38 (4): 198. https://doi.org/10.4103/0970-0218.120153.

Vázquez, Natalia, Carlos A. Rodríguez-Barrientos, Salvador D. Aznar-Cervantes, Manuel Chacón, José L. Cenis, Ana C. Riestra, Ronald M. Sánchez-Avila, et al. 2017. “Silk Fibroin Films for Corneal Endothelial Regeneration: Transplant in a Rabbit Descemet Membrane Endothelial Keratoplasty.” *Investigative Opthalmology & Visual Science* 58 (9): 3357. https://doi.org/10.1167/iovs.17-21797.

Wang, Fei, Ting-Ting Cao, and Yu-Qing Zhang. 2015. “Effect of Silk Protein Surfactant on Silk Degumming and Its Properties.” *Materials Science and Engineering: C* 55 (October): 131–36. https://doi.org/10.1016/j.msec.2015.05.041.

Wang, Fei, and Yu-Qing Zhang. 2017a. “Effects of Alkyl Polyglycoside (APG) on *Bombyx mori* Silk Degumming and the Mechanical Properties of Silk Fibroin Fibre.” *Materials Science and Engineering: C* 74 (May): 152–58. https://doi.org/10.1016/j.msec.2017.02.015.

“Effects of Alkyl Polyglycoside (APG) on *Bombyx mori* Silk Degumming and the Mechanical Properties of Silk Fibroin Fibre.” *Materials Science and Engineering: C* 74 (May): 152–58. https://doi.org/10.1016/j.msec.2017.02.015_2017.

Wang, Hai-Yan, and Yu-Qing Zhang. 2013. “Effect of Regeneration of Liquid Silk Fibroin on Its Structure and Characterization.” *Soft Matter* 9 (1): 138–45. https://doi.org/10.1039/C2SM26945G.

Watsky, Mitchell A., Mark L. McDermott, and Henry F. Edelhauser. 1989. "*In vitro* Corneal Endothelial Permeability in Rabbit and Human: The Effects of Age, Cataract Surgery and Diabetes." *Experimental Eye Research* 49 (5): 751–67. https://doi.org/10.1016/S0014-4835(89)80036-3.

Wiley, L, N SundarRaj, T T Sun, and R A Thoft. 1991. "Regional Heterogeneity in Human Corneal and Limbal Epithelia: An Immunohistochemical Evaluation." *Investigative Ophthalmology & Visual Science* 32 (3): 594–602.

Wilson, Steven E., Yu-Guang He, Jian Weng, Qian Li, Alasdair W. McDOWALL, Mark Vital, and Eric L. Chwang. 1996. "Epithelial Injury Induces Keratocyte Apoptosis: Hypothesized Role for the Interleukin-1 System in the Modulation of Corneal Tissue Organization and Wound Healing." *Experimental Eye Research* 62 (4): 325–38. https://doi.org/10.1006/exer.1996.0038.

Wongnarat, Chuleerat, and Prasong Srihanam. 2013. "Degradation Behaviors of Thai <I>Bombyx mori</I> Silk Fibroins Exposure to Protease Enzymes." *Engineering* 05 (01): 61–66. https://doi.org/10.4236/eng.2013.51010.

Wray, Lindsay S., Xiao Hu, Jabier Gallego, Irene Georgakoudi, Fiorenzo G. Omenetto, Daniel Schmidt, and David L. Kaplan. 2011. "Effect of Processing on Silk-Based Biomaterials: Reproducibility and Biocompatibility." *Journal of Biomedical Materials Research Part B: Applied Biomaterials* 99B (1): 89–101. https://doi.org/10.1002/jbm.b.31875.

Xu, Wan-Peng, Weibo Zhang, Rose Asrican, Hyeon-Joo Kim, David L. Kaplan, and Pamela C. Yelick. 2008. "Accurately Shaped Tooth Bud Cell–Derived Mineralized Tissue Formation on Silk Scaffolds." *Tissue Engineering Part A* 14 (4): 549–57. https://doi.org/10.1089/tea.2007.0227.

Yamada, Hiromi, Hiroshi Nakao, Yoko Takasu, and Kozo Tsubouchi. 2001. "Preparation of Undegraded Native Molecular Fibroin Solution from Silkworm Cocoons." *Materials Science and Engineering: C* 14 (1–2): 41–46. https://doi.org/10.1016/S0928-4931(01)00207-7.

Yang, Richeng, Peng Wu, Xinhong Wang, Zekun Liu, Cong Zhang, Yinglu Shi, Feng Zhang, and Baoqi Zuo. 2018. "A Novel Method to Prepare Tussah/ *Bombyx mori* Silk Fibroin-Based Films." *RSC Advances* 8 (39): 22069–77. https://doi.org/10.1039/C8RA03266A.

Yao, Juming, Kosuke Ohgo, Rena Sugino, Raghuvansh Kishore, and Tetsuo Asakura. 2004. "Structural Analysis of *Bombyx mori* Silk Fibroin Peptides with Formic Acid Treatment Using High-Resolution Solid-State ^{13}C NMR Spectroscopy." *Biomacromolecules* 5 (5): 1763–69. https://doi.org/10.1021/bm049831d.

Yoon, Hyeon, Eun Young Kim, Hyeongseok Kim, Chan Hum Park, Choun-Ki Joo, and Gilson Khang. 2014. "Fabrication of Transparent Silk Fibroin Film for the Regeneration of Corneal Endothelial Cells; Preliminary Study." *Macromolecular Research* 22 (3): 297–303. https://doi.org/10.1007/s13233-014-2037-6.

Zafar, Muhammad S., David J. Belton, Benjamin Hanby, David L. Kaplan, and Carole C. Perry. 2015. "Functional Material Features of *Bombyx mori* Silk Light versus Heavy Chain Proteins." *Biomacromolecules* 16 (2): 606–14. https://doi.org/10.1021/bm501667j.

Zhang, Xiaoning, Zhenyu Chen, Hong Bao, Jianwei Liang, Shui Xu, Guotao Cheng, and Yong Zhu. 2019a. "Fabrication and Characterization of Silk Fibroin/Curcumin Sustained-Release Film." *Materials* 12 (20): 3340. https://doi.org/10.3390/ma12203340.

"Fabrication and Characterization of Silk Fibroin/Curcumin Sustained-Release Film." *Materials* 12_2019 (20): 3340. https://doi.org/10.3390/ma12203340.

Zhou, Haohao, Zegong Wang, Huiqun Cao, Huiyuan Hu, Zhongkuan Luo, Xinlin Yang, Mengmeng Cui, and Li Zhou. 2019. "Genipin-Crosslinked Polyvinyl Alcohol/Silk Fibroin/Nano-Hydroxyapatite Hydrogel for Fabrication of Artificial Cornea Scaffolds—a Novel Approach to Corneal Tissue Engineering." *Journal of Biomaterials Science, Polymer Edition* 30 (17): 1604–19. https://doi.org/10.1080/09205063.2019.1652418.